行政院國家科學委員會專題研究計畫　成果報告

偶氮性染料之臭氧預處理對生物降解之影響(2/2)

計畫類別：個別型計畫
計畫編號：NSC92-2211-E-002-064-
執行期間：92 年 08 月 01 日至 93 年 07 月 31 日
執行單位：國立臺灣大學環境工程學研究所

計畫主持人：蔣本基
共同主持人：張怡怡

報告類型：完整報告
報告附件：出席國際會議研究心得報告及發表論文
處理方式：本計畫可公開查詢

中　華　民　國 93 年 12 月 23 日

1. Introduction

Textile industry is a very important industrial sector in Taiwan that contributes to domestic economy greatly. The characteristics of textile dyeing industry include large amount of water usage, the diversity of dyes and auxiliaries employed in manufacturing processes, many complicated processes used in textile industry may consume huge amount of energy, nonetheless, extensive labor force too. Although, textile industry becomes a sunset industry in Taiwan gradually, it still has the chance to transform from labor, capital, and material use intensive industry to cleaner and safer consumer product manufacturing, if we can turn the bad image of as forementioned.

Dyestuffs are the major chemicals that are widely used in coloring textiles, it not only can be used in textile, but also in the manufacturing of food, cosmetic, plastic ware, paints, and other consumer products. Since its wide application among all industries, the importance of dyes in manufacturing cannot be ignored and the caused problem needed to be fixed. The major application for dyestuffs is in textile coloring. Because dyestuff cannot be totally utilized during dye bath processes, unbinding dyestuff will be washed off in the following rinsing processes. It thus, certain amount of unused dyestuff is discharged into wastewater system. Some dyestuffs are non-biodegradable, carcinogenic, and color-persistent in water environment, that will cause visual unpleasant and may damage to aquatic ecosystem. On the other hand, the composition of textile dyeing wastewater is very complicated and it is difficult to treat. Even though adding chemicals to bring down the pollutants, the amount of sludge generation and disposal cost are not acceptable.

The ozonation application on water treatment has investigated for decades. Because of its high oxidative ability, ozone plays as a strong oxidant in water treatment, ranging from disinfection to the removal of persistent chemicals,

suggesting that ozone bears with effectiveness and completion. Many demonstrations have proven its feasibility in water treatment. Some researchers have studied the alternative of ozone on wastewater, hazardous waste, and chemical reaction kinetics in recent years, numerous research papers have published and indicated that ozone may serve as a important agent in many field of treatment. Because of the high oxidation strength, the COD and impurities in wastewater can be oxidized and decolorized, ozonation can make up the deficiency of secondary treatment as well. Some investigators have viewed ozonation as a promising technology followed after nanotechnology in next decade.

2. Literature Reviews

2.1 Colorant

Colorant is the one of major components that cannot be ignored during colorization processes. Depending on its solubility and the affinity between fiber and dyestuff, colorant can be divided into dyestuff and pigment. Usually, dyestuff can dissolve homogeneously or highly diffusive in water that can color the fiber evenly. For the pigment, usually it does not come with the affinity with water or fibers, it needs chemicals, such as adhesives and binders, to let pigment fix on fiber or other surfaces.

Colorant can be divided into two categories as: natural and synthetic products. Natural dye can be extracted from minerals or plants. There are evidences that show human being had applied mineral dye in painting or drawing before history. Until 1856, a British chemist Dr. W.H. Perkin used the based material from coal tar oil to synthesized quinoline. By accidentally, Dr. Perkin discovered mauvein (a basic dye), a kind of purple colored material. In 1860, Dr. Perkin successfully synthesized aniline blue. Since then, the research on synthetic dye was booming in England and to rest of world (Dyeing & Finishing).

Synthetic dye may base on the application or its chemical structure. Usually, the dye users prefer the way of categorization by its application. Thus, it was illustrated in Table 2.1

Table 2.1 the category of dye by its application

Direct coloring	Direct dye
	Acid dye
	Base dye
	Mordant Dyestuff

Mordant coloring	Mordant Dyestuff
Reductive coloring	Vat dyes Acid Mordant Dyestuff Gabrian Sulphur
Color illusending	Naphthol Dye
Disperse coloring	Disperse dye
	Reactive dye Florescent whitening dye Oily dye Pigment

The dye can be categorized by its chemical structure that include 21 different structures that are shown in Table 2.2:

Table 2.2 Chemical structures

Nitroso	Nitro	Mono-azo	Di-azo
poly azo	Stibene	Diphenyl methane NH	Triaryl methane
Xanthene	Acridine	Quinoline	Methine
Thiazole	Indamine	Azine	Oxazine
Thiazine	Carbonium	Indigoid	Anthraguinone
Phthalocyanine			

2.2 Azo dyes

Azo dye is a kind of synthetic organic dyes that contain nitrogen as the azo group -N=N- as part of their molecular structures which links two sp hybridised carbon atoms (as part of aromatic atoms); more than half the commercial dyes belong to this class. Depending on other chemical features, these dyes fall into several categories defined by the fibres for which they have affinity or by the methods by which they are

applied (Encyclopædia Britannica). They are manufactured from aromatic amines by azo coupling reaction that may occur under room temperature. Most azo dyes contain only one azo group, but some contain two (disazo), three (trisazo) or more. In theory, azo dyes can supply a complete all range of colors. But practically and commercially, they tend to supply more yellows, oranges and reds than any other colors.

Azo dyes exhibit bright, high intensity colors, more than the anthraquinones, a next most common dye been used; they have good fastness properties, but not so good as the carbonyl and phthalocyanine dyes, they are applied in printing, painting, plastics, color printing, stationary, rubber, and leather processing. Azo dyes are inexpensive comparing to other classes of dyes that may due to the processes involved in manufacture. Furthermore, the simplicity of the reactions, low energy requirements for the reaction, all reaction carried out in water maybe the key issues for azo dye to compete with other dyes based on the cost. So far, there are more than 2000 commercialized dyes of which half are azo dyes (Chu et al, 2000). Since, dyestuff is applied in industries widely, they become one of important materials that cannot be ignored in product manufacturing.

As forementioned, the dyestuff applied in textile industry may include acid, basic, azo dye etc., and the azo dyes are the most important dye among them because of the consumption amounts. The amount of dye production in Taiwan increased from 35 kilotons in 1991 to 69 kilotons in 2001 (Statistic Department, 2002).

The reason for dye illuminating is because it bears with illuminating groups, Hao (2000) had concluded the illuminating groups of azo dyes as shown in Table 2.3.

Table 2.3. The structure of illuminating groups of azo dyes

Structure	Color

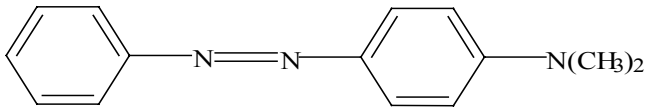	Yellow-Green
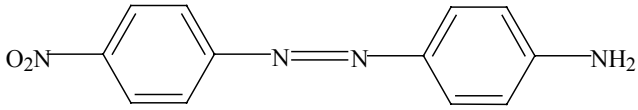	Yellow
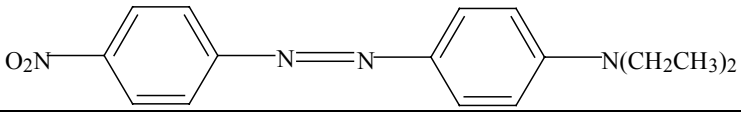	Red
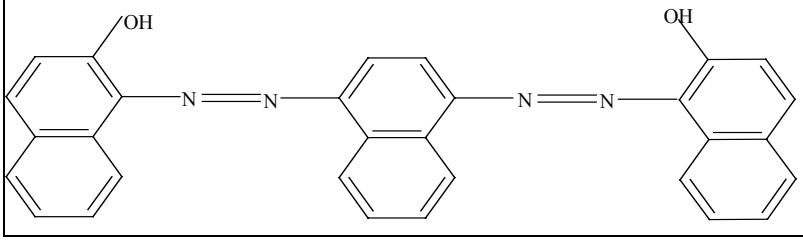	Blue

During textile dyeing process, many chemicals, such as $NaCO_3$, NaCl, and $NaCO_3$, have been added into reactors, even may added surfactants as add or for the purpose of impurities removal, following are the typical structures of surfactants that have been used in textile dyeing process normally (Shenai, 1976) and shown in Table 2.4:

Table 2.4 The common surfactants used in textile dyeing process

Chemical	Structure
Aniline	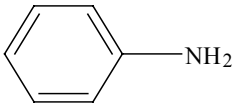
Soap	3R-COONa
Nonyl phenol-ethylene oxide	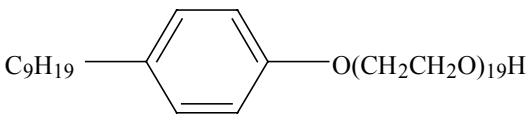

2.3 The use restriction of azo dye

In the announcement of European Parliament Directive 2002/61/EC, the European Union (EU) had decided that azo dyes in consumer goods had to be enacted. Because azo dyes contain one or more nitrogen-nitrogen double bonds in their chemical structure, under reductive conditions and using sodium dithionite, these azo groups can be cleaved to form two amines, shown as follows:

The chemical groups A and B are aromatic or aryl species in order to stabilize the electron structure and absorb light in the visible range, so the amines formed by cleavage of the azo group will obviously be aromatic amines. A small number of the aromatic amines are classified as carcinogenics or potentially carcinogenics to humans. Table 2.5 lists 22 aromatic amines. Further one of the most recent amines added to the list is 4-aminoazobenzene, which in itself contains an azo group (European Union, 2003).

Table 2.5 List of aromatic amines according to the EU Directive 2002/61/EC.

No.	Substance	CAS number
1	4-aminodiphenyl	92-67-1
2	benzidine	92-87-5
3	4-chloro-o-toluidine	95-69-2
4	2-naphthylamine	91-59-8
5	4-amino-2',3-dimethylazobenzene	97-56-3
6	2-amino-4-nitrotoluene	99-55-8
7	4-chloroaniline	106-47-8
8	2,4-diaminoanisole	615-05-4
9	4,4'-diaminodiphenylmethane	101-77-9

10	3,3'-dichlorobenzidine	91-94-1
11	3,3'-dimethoxybenzidine	119-90-4
12	3,3'-dimethylbenzidine	119-93-7
13	3,3'-dimethyl-4,4'-diaminodiphenylmethane	838-88-0
14	4-cresidine	120-71-8
15	4,4'-methylene-bis-(2-chloroaniline)	101-14-4
16	4,4'-oxydianiline	101-80-4
17	4,4'-thiodianiline	139-65-1
18	2-aminotoluene	95-53-4
19	2,4-diaminotoluene	95-80-7
20	2,4,5-trimethylaniline	137-17-7
21	2-methoxyaniline	90-04-0
22	4-aminoazobenzene	60-09-3

2.4 The ozone characters

Ozone is a gas with the property of low solubility and high reactivity that can oxidize organics and kill pathogens, it has been applied in many fields including drinking water and de-odor treatment. It is gaseous and colorless under room temperature but with strong smell which can be detected under very low concentration (0.02－0.05 ppm). Nonetheless, ozone (2.07 eV) is a strong oxidant and its oxidation ability is next to the hydroxyl free radicals (·OH), 2.8 eV. As dissolved in water, ozone will stimulate the formation of ·OH that will react with organics or inorganics in water. As a result, the pollution level can be reduced and color remaining in water can be removed too.

Ozone will self-decompose into oxygen in water that may not cause pollution problems when apply ozone treatment to water. Under 20 ^{o}C, the solubility is only 570 mg/l whereas the solubility for chlorine gas is about 12 times of ozone. In general, the ozone concentration generated from ozone generator usually is less than 14 % (V/V) that may restrict the transportation between gas and liquid phases. Thus,

residual ozone concentration in water treatment ranges from 0.1 to 1 mg/l. Higher dissolved ozone concentration may happen only if under better mass transport conditions. Langlais et al. (1991) had reported that ozone solubility will decrease as temperature increasing that can apply to all cases of gas dissolve in water, and it is affected by $[H^+]$ and ionic strength, a regression was proposed as:

$$\ln(H_A) = 0.45 + 0.043T\ (^oC) \quad (1)$$

Per ozone decomposition, Qiu (2001) employed batch reactor to study the decomposition of ozone, under 25℃, the concentration of OH group has positive relationship with ozone reaction rate constant, which shows as first-order reaction:

$$k_d = 20[OH^-]^{0.5} + 900[OH^-] \quad (2)$$

Gurol and Singer(1982) focused on the study of ozone decomposition in pure water and proposed following equation:

$$r_{O3} = k_d[O_3]^2 \quad (3)$$

Gurol gave the k_d definition as rate constant and ionic strength and the pH value of buffer solution can affect k_d value.

Some other researcher (Ku et al, 1996) used bubble column to analyze the decomposition behavior of ozone in water and proposed the equation as:

$$-d[O_3]/dt = 23.47[O_3]^{1.5}[OH]^{0.359} + 0.1414[I_{uv}]^{0.9}[O_3]^{1.5}[OH]^{0.064} \quad (4)$$

2.5 Mass transfer

Soleto used two film theory to illustrate the phenomena of ozone in liquid and gas phases under steady state, and the mass balance of ozone can be expressed as:

$$\frac{d[O_3]}{dt} = k_{LO3}a\left([O_3]^* - [O_3]\right) - k_A[O_3] - k_b[OH^-]^{0.5}[O_3]^{1.5} \quad (5)$$

Cogo et al. (1999) proposed the ozone concentration in gas phase (C_G) and liquid phase (C_L) shall have linear relationship as expressed as

$$C_G = mC_L^* \quad (6)$$

When quantified ozone mass transfer, Cogo proposed following equation:

$$\frac{dC_L}{dt} = k_1 a\left(C^*_L - C_L\right) \quad (7)$$

Other researcher, Andreozzi (1999), used para-chlorophenol (CHP) as research target and emploted Hatta's Number as the way to describe mass transfer

$$Ha = \sqrt{\frac{D_{O_3} zkC^0_{in}}{\left(k_L^o\right)^2}} \quad (8)$$

where

z = ozone coefficient，

k = the ozonation rate constant of CHP

k_L^0 = mass transfer coefficient in gas phase

C_{In}^0 = para- CHP initial concentration

D_{O3} = dispersion coefficient of ozone in water

Ha = Hatta's Number

Under the conditions of $Ha < 2.0$ and $Ha > 25$, Andreozzi proposed the reaction

equation for CHP and ozone as:

$$\text{para-CHP} + z\text{O}_3 \rightarrow \text{products} \quad (9)$$

Also, Andreozzi proposed the mass transfer relationship between ozone and CHP as following:

$$\frac{d[O_3]_B}{dt} = \frac{Q}{V_B}([O_3]_{in} - [O_3]_B) - \frac{k_L{}^0 a[O_3]_B \alpha E}{V_B} V_L . \quad (10)$$

$$\frac{d[O_3]_F}{dt} = \frac{Q}{V_F}([O_3]_B - [O_3]_F) \quad (11)$$

$$\frac{d[CHP]}{dt} = -\frac{k_L{}^0 a[O_3]_B \alpha E}{z} \quad (12)$$

Where V_B = bubble volume

V_F = freeboard volume

V_L = reaction volume

t = reaction time

$[O_3]_{in}$ = the initial concentration of ozone in gas phase

$[O_3]_B$ = the volume of ozone bubble

$[O_3]_F$ = ozone freeboard volume

α = Ostwald coefficient

E = enhance factor

Beltràn employed semi-batch reactor and introduced ozone/UV, ozone/ H_2O_2 or H_2O_2/UV to study and define enhance factor (E) as:

$$E = \frac{m_i - m_0}{k_L a C_{O_3}{}^* V} \quad (13)$$

Where E was the enhance factor, m_I and m_0 are the ozone molar flow rate of inflow and outflow respectively.

k_La = volumetric coefficient of mass transfer

C^*_{O3} = the ozone equilibrium concentration in water

V = reaction volume

D_{O3} = dispersion coefficient of ozone ($1.3\times10^{-9}m^2s^{-1}$)

D_I = dispersion coefficient of solute ($10^{-10}m^2s^{-1}$)

k_L = mass transfer coefficient in liquid phase ($3\times10^{-4}m^2s^{-1}$)

k_d = reaction rate constant

Then, Beltràn defined the efficiency of ozonation (E_f) as:

$$Ef = \frac{m_i - m_0}{m_i} \times 100 \tag{14}$$

and, the stochiometric of ozonation, z, will as

$$zO_3 + M \rightarrow \text{Products} \tag{15}$$

$$z = \frac{3200}{(COD_0 - COD)V}(m_i t - q_t) \tag{16}$$

where, COD and COD_0 represent the concentration in the time t

q_t = molar number of ozone under time t

Beltràn found out, no matter what condition had been conducted, z almost is a certain value, which locates between 1 and 2.

2.6 Reaction kinetics

Ozonztion reaction can be categorized as two groups, one is direct reaction and

the other is indirect reaction, ozone can produce OH• groups and that free radicals can react with reactant directly. The reaction mode can be shown as following

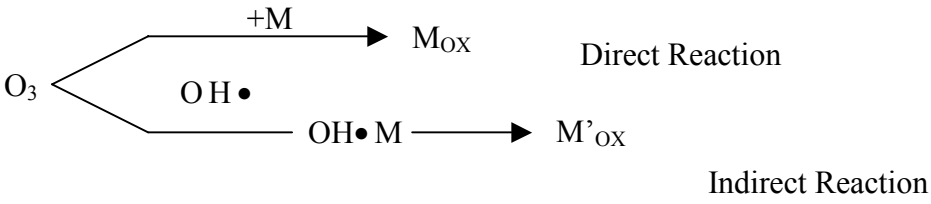

Langlais et al. (1991), Beltràn et al. (1992), and Parishena et al. (2000) all proposed ozone could react with organic matters (M) and could be classified as a first-order reaction. Its reaction mechanisms are:

$$O_3 + M \xrightarrow{k_1} \text{products} \quad (17)$$

$$O_3 + M \xrightarrow{k_2} OH\bullet + \text{products} \quad (18)$$

$$M + OH\bullet \xrightarrow{k_3} \text{products} \quad (19)$$

$$M + OH\bullet \xrightarrow{k_4} OH_2\bullet + \text{products} \quad (20)$$

Where the ks value represent the reaction rate. Hermanowicz (1999) proposed ozone decomposition could be described as first-order reaction kentics. Under batch reaction, the ozone decomposition were 0.2-4orders or n-th order kinetics.

For the decolor of dyeing water, Arslan (2000) used reactive dyes, Procion Yellow HE4R and Black SB, as target compounds and proposed following reaction kinetics equations:

$$\frac{-dCOD}{dt} = K_{COD} COD \quad (21)$$

where $K_{COD} = K$[COD]

2.7 Biodegradation

Usually, the biodegradation of azo dye in wastewater was difficult to be enhanced without any further oxidation. Haug (1991) and Wuhrmann (1980) stated, no matter under aerobic or anaerobic conditions, it is difficult to employ biological treatment to treat textile dyeing wastewater alone.

As mentioned, the oxidation of azo dyes may produce amines that were toxic to aqueous ecosystem, nonetheless the activated sludge system. Ozonation may serve as an important and promising method in enhancing the biodegradation of azo dye that would benefit to the following treatment units. Hao et al. (2003) had pointed out ozone treatment could reduce COD and color significantly; the BOD would be enhanced too. It thus, the BOD_5/COD values usually would larger than 0.1, indicating that the biodegradable organics increased after ozone treatment. Because of the structures of azo dyes, as described previously, it is difficult to use biological treatment to deal with wastewater that containing azo dyes.

O'Neill (1999) paper revealed that under the condition of without ozonation treatment unit, and to study the aerobic or anaerobic treatment processes of Procion Red H-E7B. O'Neill employ USAB reactor and inner-circulated digestor (ITD) to study the biodegradation of reactive dyes. He found out under the aerobic condition, COD and BOD removal rates could reach 347 and 71% respectively of 57 days, but no color removal function.

2.8 Ozonation vs. Biodegradation

Beltràn (1999) employed continuous activated sludge system combine with ozone/UV treatment to treat municipal sewage, he observed the COD and BOD/COD changes in activated sludge unit. As the results, he stated that if without adding post ozonation unit and retention time equaled to 5 hours, the COD removal rate was 59.1%, MLVSS was 37.2%, and BOD/COD was 0.16. But, if adding post ozonation unit, COD and MLVSS degradation ratio could reach 71 and 78.4%, respectively, and BOD/COD could be raised to 0.36. To sum up, post ozonation unit combined with continuous activated sludge system could treat municipal wastewater and reach

excellent results, other than that, post ozonation unit could reduce the concentration of total nitrite and benefit to biological treatment.

3. Materials and Methods

The experimental setup in this study can be divided into two systems, one is semibatch system and the other is continuous countercurrent bubble column system. Different azo dyes are applied in both systems to investigate the reaction kinetics, mass transfer efficiency, decolorization, and mineralization under various designed conditions.

3.1 Material

The target compounds used in this study included Acid Orange 6, AO 6, was provided by Sigma-Aldrich and Reactive Black 5, RB 5, was provided by Yi-Hwa Co., both structures were shown in Fig. 3.1. Both target compounds used without further purification. The physical and chemical properties of both compounds were shown in Table 3.1.

The chemicals for COD, TOC, and BOD5 were purchased from Sigma-Aldrich.

(a) AO 6

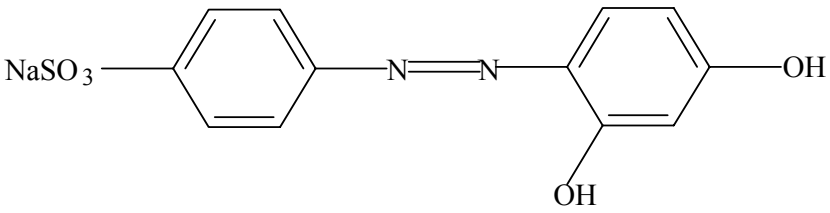

(b) RB 5

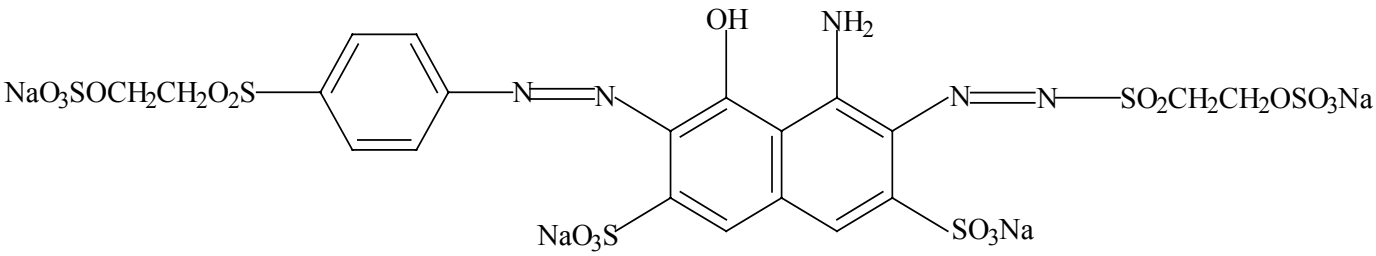

Figure 3.1 The chemical structures of (a) AO 6 and (b) RB 5.

Table 3.1. Physical and chemical characterizations of AO 6 and RB 5

Property	Acid Orange 6	Reactive Black 5
Class	Monoazo	Disazo
Maximum wavelength (λ_{max})	490 nm	597 nm
Molecular formula	$C_{12}H_9O_5SN_2Na$	$C_{26}H_{21}N_5Na_4O_{19}S_6$
Molecular weight (g/mol)	316	991
		Under [Dye]= 75 mg/L:
COD (mg/L)	188	76
TOC (mg/L)	77	11

3.2 Experimental design and setup

The experimental design consideration for ozonation reactors in this research can be divided into two systems that are bubble column and semi-batch reactor. The unique characteristics of two systems are that comprises three major parts: feeding system, reactor, and monitoring system. The design considerations are quite different between to systems and illustrated as following sections.

3.2.1 Semi-batch system

Semi-batch reactor for ozonation is a typical and effective instrument to study reaction kinetics and Henry's constants. The reactor design is followed McCabe, et al. (1993) a standard 6-bladed-disk turbine design and made of Pyrex glass, with an inner diameter of 17.2 cm (effective volume of 5.5 liters), and equipped with a water jacket to maintain a constant solution temperature of 25 ^{o}C. The cylindrical gas distributor with a pore size of 10 μm was located at the bottom of the reactor. The total sampling volume is less than 5% of total reaction volume to minimize the affect

of sampling on reaction.

The ozone was generated from pure oxygen in an ozone generator (model SG-01A, Sumitomo, Tokyo, Japan) that ozone-enriched gas was conducted from the distributor at the reactor bottom, and the feed rate might be controlled by a precision flow control meter (Cole-Parmer, MI, USA). The apparatus was shown in Fig. 3.2.

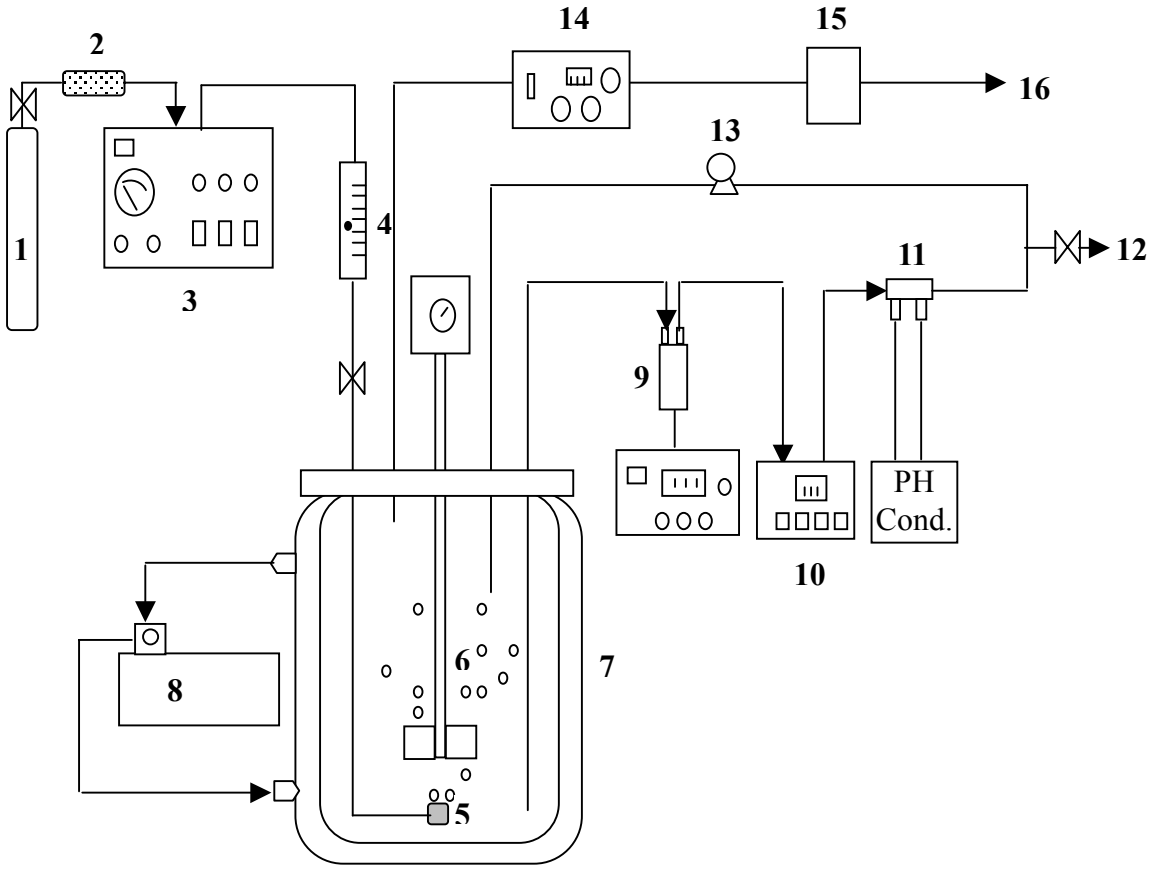

Figure 3.2 The experimental apparatus sketch of stirred reactor.

Components: 1. Oxygen cylinder, 2. Desiccative tube, 3. Ozone generator, 4. Digital flow meter with precision control, 5. Ozone gas distributor, 6. 6-bladed-disk turbine, 7. Reactor, 8. Thermostat, 9. Liquid ozone sensor, 10. Photospectrometer, 11. pH and conductivity sensors, 12. Sampling port, 13. Circulation pump, 14. Gaseous ozone detector, 15. Washing bottles with KI solution, 16. Ventilation.

3.2.2 Countercurrent bubble column

Fig. 3.3 shows the schematic diagram of ozone contacting bubble column. The column is made of PVC, 3.5-m high and 14.2-cm inner diameter, was operated in the countercurrent mode with water flowing downward and gas flowing upward. The upright bubble column was pre-customized and equipped with 7 sampling ports with ball valves. An overflow pipe was connected to column to prevent water overflowing into off gas monitoring instruments.

A stainless steel (SS 316) sparkle was facilitated on the top of column that was mounted on the cap. At the bottom, a ceramic filter plate was used to serve as gas distributor that average pore size was about 50 μm. Ozone-enriched gas was pumped through a one-way valve (Swiglog) and enter into bubble column system that could resist the pressure up to 3000 psi. The gas flow rate was controlled by a flow meter with precision control (Cole Parmer). Ozone gas and water were both introduced continuously into the contactor. Ozone-containing gas was generated with pure oxygen by a Sumitomo SG-01A generator and introduced into the column that mixed gas flowed through a ceramic diffuser located at 10 cm from the bottom of the contactor.

A circulation pump (IWAKI, Tokyo, Japan) with Teflon wet part was added to the system for further experiment on semibatch type. Effluent was discharged from the bottom of column that was conducted into sewer system, a pin valve with Teflon wet part was used to control the effluent discharge rate as well as the maintain the liquid level during the experimental course.

The liquid-storage tank was equipped with the thermostat to maintain a constant temperature of solution at 25 ^{o}C in all experiments, and a stirring system to keep the solution homogeneously throughout the experimental courses.

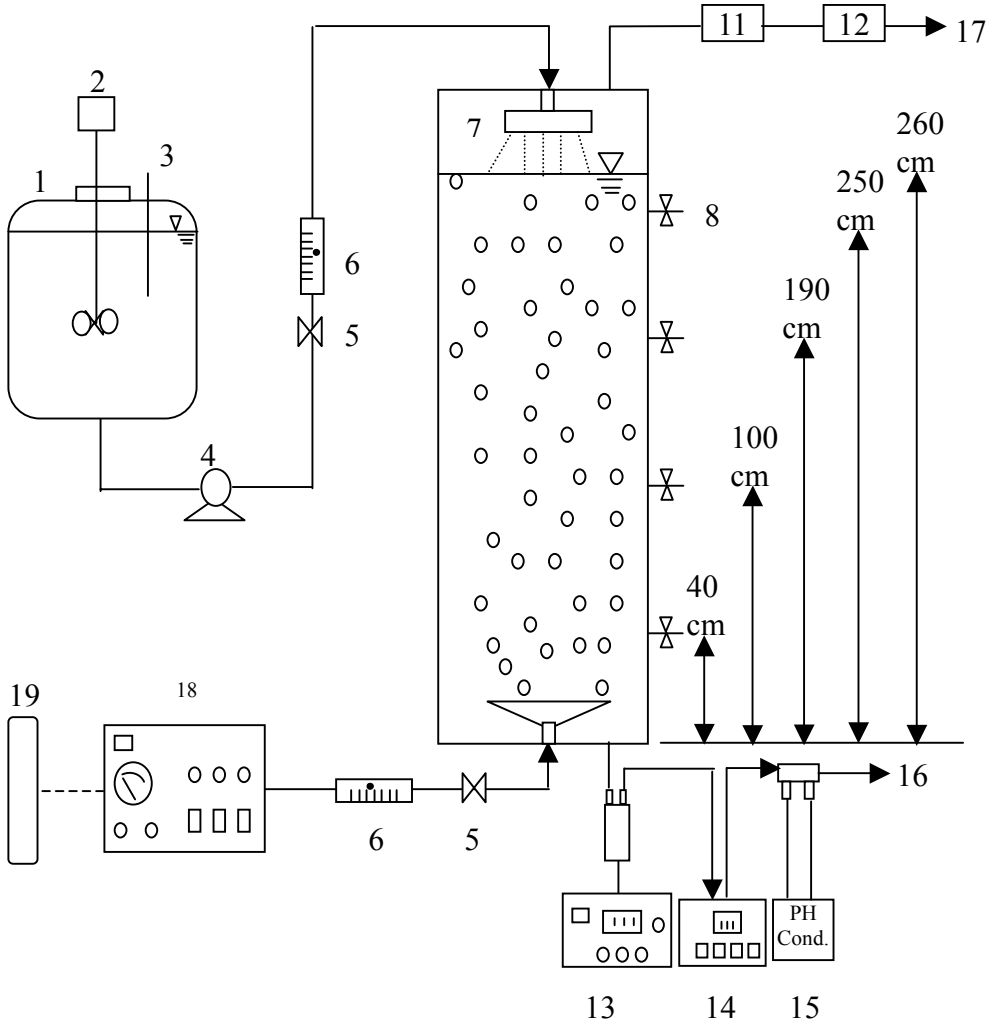

Figure 3.3 Experimental setup. The denoted numbers on above figure are described as follows: 1. Water Tank, 2. Stir, 3. Water leveling meter, 4. Thermostat w/ temperature controller, 5.Drainage, 6.Pump, 7. Flow control valve w/ PID control, 8. Digital flow meter, 9. Pressure transmitters, 10. Sparkle, 11. Bubble column reactor (300 × 12.5 ID), cm, 12. O_3 gas distributor, 13. Sampling ports, 14. Sensor box (fitted with pH, DO, Conductivity, dissolved O_3), 15. O3 gas detector, 16. O3 gas destroyer and 17. Vent to hood, 18. Ozone generator, 19. Oxygen supply.

3.3 Experimental procedures

3.3.1 Semibatch system

Before starting a semi-batch experiment, following steps were preceded:

1. Prepare [AO 6] = 200 mg/L of stock solution for further experiments that may depend on the requirement to add buffers into solution, that buffers were comprised with the combination of phosphates.
2. Turn on the thermostat to maintain the desire temperature such as 15, 20, 25, and 30 ^{o}C, and wait for the state become steady; that may need about 60 min.
3. Turn on ozone generator (Sumimoto SG-10A) and set the ozone generation node to certain mark that was pre-tested by directed ozone-containing gas to an ozone monitor (model 1008-HC, Dasibi, CA, USA), which was previously calibrated with the KI solution.
4. As the ozone concentration kept steady, turn the three way valve and let ozone-enriched gas bubbled into the solution that was prepared beforehand.
5. Meanwhile, record the monitoring data shown on the pH (Suntex), conductivity (Suntex) and the visible light spectrum (model Cintra 20, GBC Scientific Equipment, Australia).
6. A dissolved ozone monitor (model 3600, Orbisphere Laboratory, Switzerland) with a membrane-containing cathode sensor was used for the analysis of dissolved ozone concentration.
7. At certain time interval, sample was draw from reactor for further parameters testing.

3.3.2 countercurrent bubble column reactor system

In this experiment, stock solution was prepared by dissolving RB 5 (75 mg/L) into water that was stored in a water tank. The solution temperature was kept at

25^{o}C and the stir was on during the experimental runs. Follow the step 3 to 7 described in section 3.3.1. As experiment initiated, the steps for ozone generation, monitoring, and data collection were similar to semibatch system. It was very important to maintain the liquid level at 2.6 m throughout the experimental runs. The sampling was different to the semibatch system. Because the column height may refer to the contacting time of ozone with RB 5, thus, the samples were draw from bubble column system not only at effluent port but also from the sample port of four different height, 0.4 m, 1.0 m, 1.9 m, and 2.5 m. A set of monitors, including pH, conductivity, ORP, dissolved ozone sensor, and the absorbance of visible wavelength, were facilitated and the data was recorded.

3.4 Analytical Method

The analytical methods used in this study can be divided into following groups.

1. Ozone gas was determined by bubbled through a 250mL capacity gas wash bottle filled with 2% potassium iodide (KI) solution, then, titrated with sodium thiosulfate ($Na_2S_2O_3$) according to APHA. The off-gas is monitored by an ozone analyzer (Dasibi model 1008-HC, California, USA) and calibrated by 2% KI solution as well.
2. The liquid dissolved ozone concentration is monitored by a liquid ozone monitor (model 3600, Orbisphere Laboratory, Neuchàtel, Switzerland) that equipped with a membrane-containing cathode sensor to analyze dissolved ozone concentration, and calibrated by the indigo method which are described in APHA.
3. The absorbance of λ597 nm (A597 nm) and UV254 is performed by a UV-Visible detector (model Cintra 20, GBC Scientific Equipment, Victoria,

Australia). The visible wavelength absorbance was examined by using wavelength scanning from 400 to 700 nm and integrated the area, expressed as integrated absorbance unit (IAU), under absorbance curve. The IAU is proportional to sample color which has been mentioned in previous study (Wu and Wang, 2001).

4. The UV254 absorbance was followed the method described in Standard Methods section 5910.
5. The calibration for dye concentration, AO 6 as an example. Take 6 different AO 6 concentrations and used UV-Visible detector to scan the absorbance from 200 nm to 900 nm, the results were shown in Fig. 3.4. It was found that there were two significant absorbance peaks appearing at 254 nm and 385 nm, indicating that the absorbance peak at 254 nm represented the existing of aromatic compound. For the [AO 6] = 0 – 50 mg/L, the scanning was shown in Fig. 3.5 indicating that the well distribution of absorbance peak at 385 nm and with low noise signals.

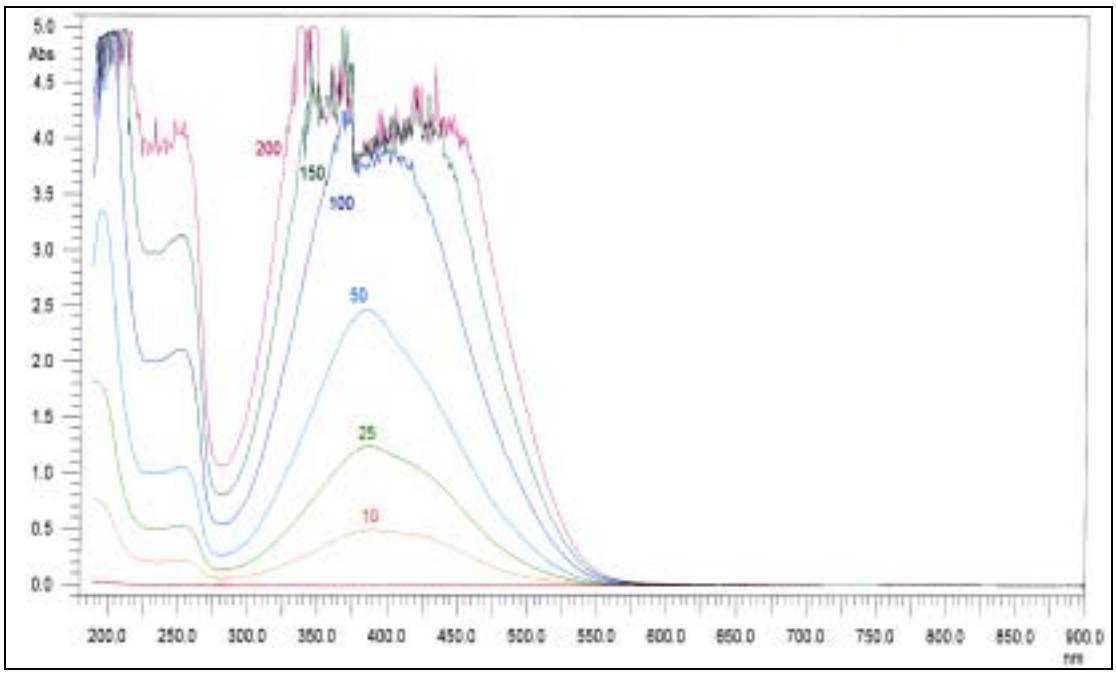

Figure 3.4 The UV – visible wavelength scanning (200 nm to 900nm) for different AO 6 concentration ([AO 6]＝0 to 200 mg/L)

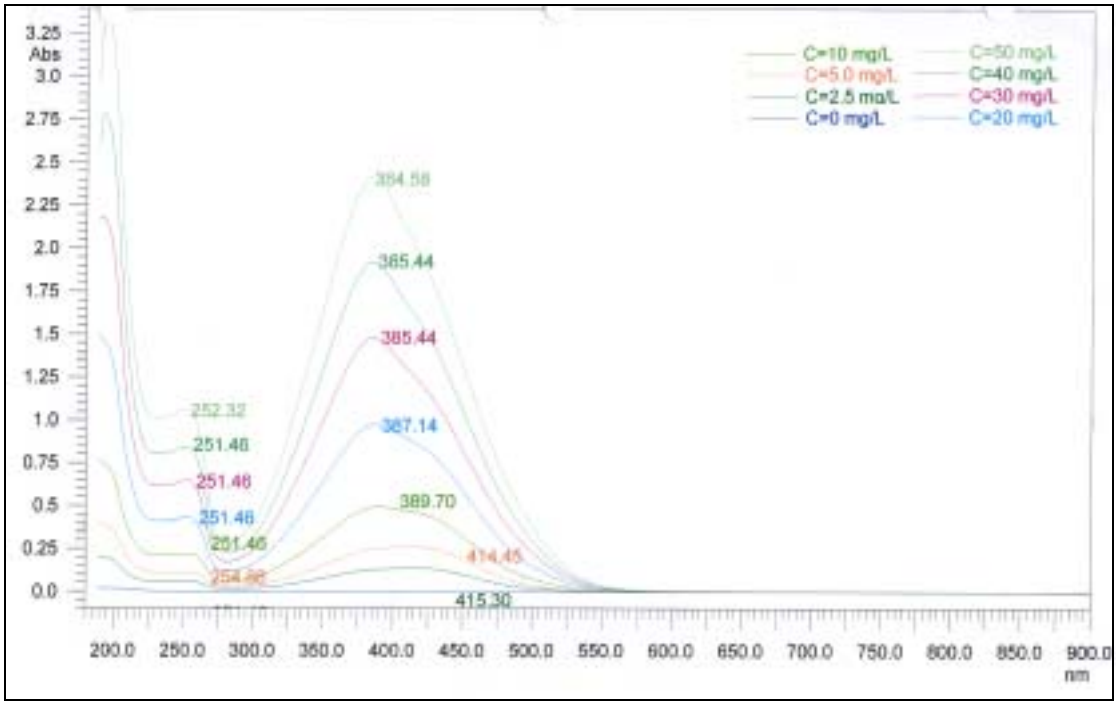

Figure 3.5 The UV – visible wavelength scanning (200 nm to 900nm) for different AO 6 concentration ([AO 6]＝0 to 50 mg/L)

6. The COD for the ozone treated and untreated dye solution were determined by APHA/AWWA/WCF Standard Method.
7. A TOC analyzer (model 1010, O.I Corporate, USA) was employed to analyze the TOC concentration, the referring document could be found in Standard Methods section 5310.
8. An ion analyzer (Capillary Ion Analyzer, Waters, USA) for the anion analysis.
9. The BOD5 testing was following the method described in NIEA W510.53A and sludge was provided by Na-Hu sewage treatment plant.
10. Toxicity test was used the commercialized test kit to measure the 50% of effective concentration (EC50) for the samples. The Microtox test kit contains marine luminescent bacteria, Photobacterium phosphoreum, florescent monitor (model m500, AZUR Environmental), diluents. Microtox is the worldwide standard for rapid and accurate toxicity monitoring.

3.5 Tracer test

The tracer test was intended to understand the performance and flow conditions in bubble column. The test protocol was illustrated as follows:

1. Adjust the liquid level to preset height, then, adjusting the gas flow rate and continue to 3 times of hydraulic retention time (HRT).
2. Preparing the NaCl solution ([NaCl] = 100 g/L) and producing the NaCl concentration calibration.
3. Injecting the NaCl solution (about 10 mL) from the top of bubble column, meanwhile count up the time from the injection. After 10 seconds, collecting the samples from the exit of bubble column.
4. Measuring the conductivity of each sample.

4. Results and Discussion

4.1 The parameters of water quality for AO 6 and RB 5

The parameters of water quality for the oxidation of AO 6 by ozone was conducted in a semi-batch system. The results were as follows:

4.1.1 Decolorization and mineralization of AO 6 by ozonation with UV irradiation

As mentioned, one AO 6 molecule contains one azo bond that is easily been destroyed by ozone. Breaking the azo bond may disable the function of chromophores and decolorization may be enhanced. Thus, to observe the parameters change may explain the way of ozonated AO 6 and related mechanisms. In order to compare the difference between O_3 alone and O_3 with UV irradiation (15 and 30W/m^2), both systems will be discuss in the following section.

4.1.2 Variations of pH, A_{max}, and Color

The results of pH, conductivity, A_{max}, and color under the experimental conditions of O_3 alone and O_3/UV are shown in Fig. 4.1. As ozonation proceeded, due to organic and inorganic acids formation, the pH decreased rapidly. The pH gradually reached a stable value when organic acids were oxidized.

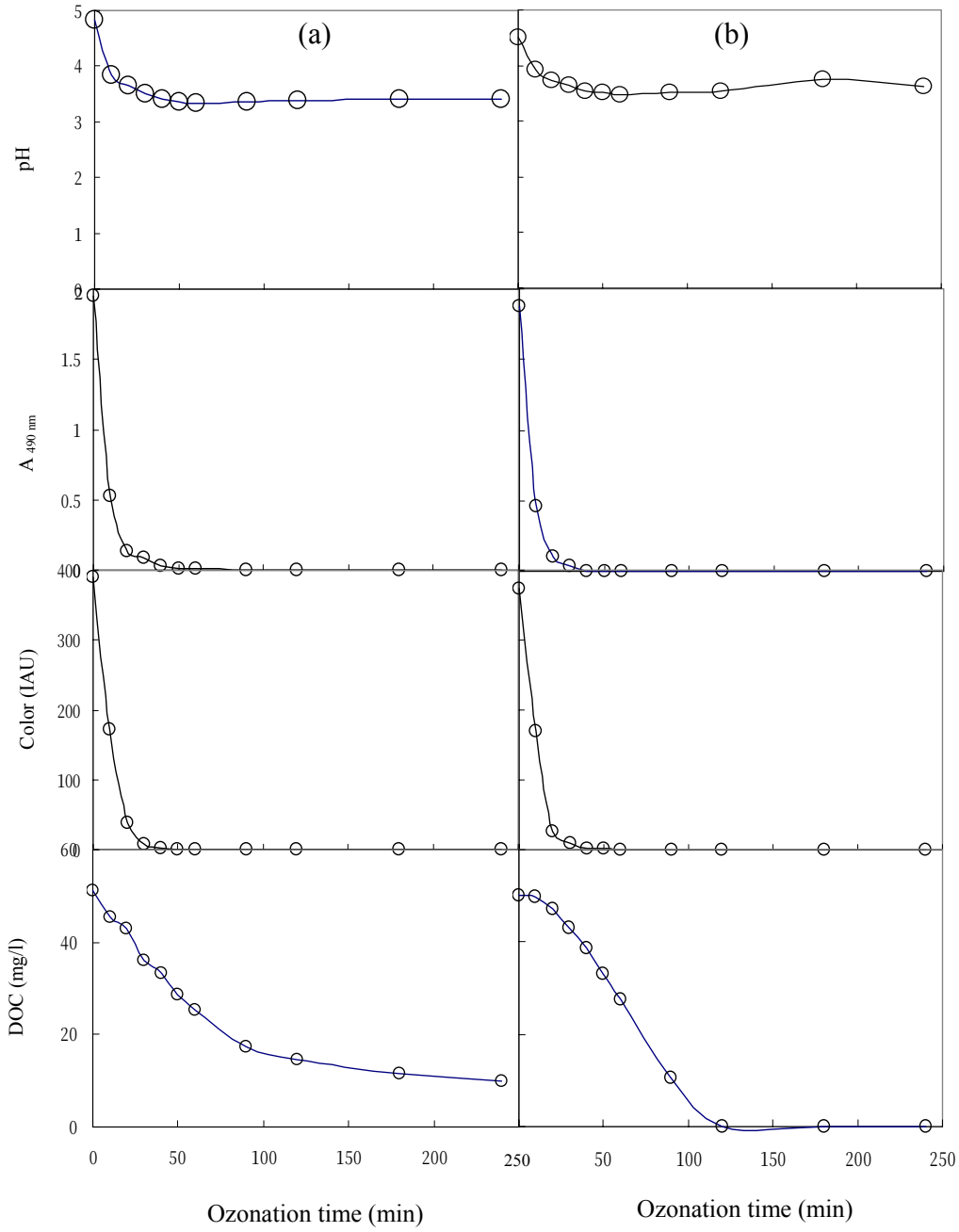

Figure 4.1. Concentration profile of pH, A_{max}, and color of AO 6 in a semibatch system. (a) O_3 = 18.7 mg/l-min, (b) O_3 = 18.7 mg/l-min with UV intensity 30 Wm^{-2}. (Initial [AO 6] = 0.2 g/l, pH = 4.7±0.1, TOC = 52±2 mg/l, IAU = 390±10, gas flow rate = 2.1 l/min, 25 ^{o}C).

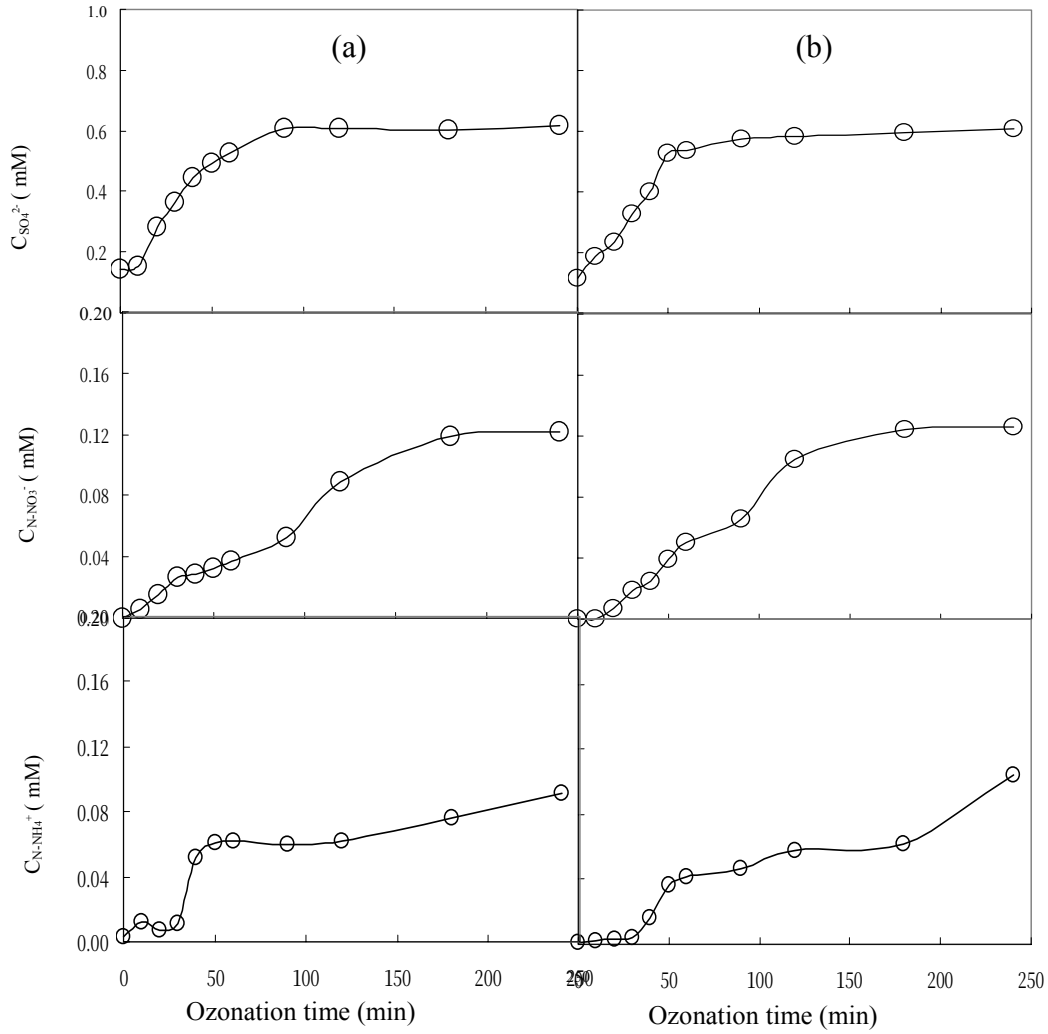

Figure 4.2 Concentration profile of DOC, SO_4^{2-}, NO_3^-, and NH_4^+ of AO 6 in a semibatch system. (a) O_3 = 18.7 mg/l-min, (b) O_3 = 18.7 mg/l-min with UV intensity 30 Wm^{-2}. (Initial [AO 6] = 0.2 g/l, pH = 4.7±0.1, TOC = 52±2 mg/l, IAU = 390±10, gas flow rate = 2.1 l/min, 25 ^oC).

The AO 6 species disappeared gradually as observing its absorbance at 490 nm, the specific wavelength ($A_{490\ nm}$). It is noted that the disappearance of AO 6 followed a pattern almost the same for the O_3 alone and the O_3/UV system. As ozonation continued, after 20 min, the rates of AO 6 consumption were much slower than the initial rates, and AO 6 species diminished to undetectable level within 30 min. The reaction time for the total decolorization in both the O_3 alone and the O_3/UV systems was almost the same at an O_3 dosage of 18.7 mg/l-min (Figs. 4.1a and 4.1b); the color disappeared at about 50 min. It, thus, suggested that the contribution of UV irradiation to decolorization was not important. The •OH radicals generated by UV are non-selective oxidizers, and under acidic conditions, lesser amount of •OH radicals would produce and compete with dissolved O_3 in reacting with organics. As a result, the contribution of •OH to the decolorization was not significant. It can be concluded that dye molecules with azo bond (N=N) were easily destroyed by ozone and generated intermediate products.

The theoretical TOC at AO 6 concentration of 200 mg/l was 92 mg/l. Since AO 6 has a 65% purity, this yield an initial TOC of 60 mg/l. The observed initial DOC (at AO 6 = 200 mg/l) in this study was 54 $\pm$ 2 mg/l, less than the purity-corrected theoretical TOC. The difference between theoretical and observed value was not remarkable. DOC reduction in the O_3/UV system proceeded faster than the O_3 alone system. Within 120 min, DOC approached zero in the O_3/UV system (Fig. 4.1b), while still remained even after 240 min in the O_3 alone system (Fig. 4.1a). That result clearly indicated that the contribution of UV irradiation on catalyzing O_3 to produce free radicals was remarkable in removing ozonation by-products. For example, the DOC removal rates for the O_3 alone and the O_3/UV systems were 0.36 and 0.61 within first 50 min and between 50 and 90 min respectively, at an ozone dose of 0.92 mg/l-min. Evidently, after complete of decolorization (t = 50 min), the DOC

reduction rate was enhanced because most ozone was used to mineralize intermediate products. The results also suggested the remarkable contribution of UV irradiation on mineralization of persistent intermediate products. Pseudo-first order reaction pattern could explain DOC reduction as well as decolorization and the disappearance of AO 6 species.

4.1.3 Sulfate, nitrate, and ammonium formation

Referring to the chemical structure of AO 6, one AO 6 molecule contains one sulfate group and the purity-corrected theoretical sulfate concentration at the end of total minerization should be 0.41 mM. As shown in Fig. 4.2a and 4.2b, sulfate ($C_{SO_4^{2-}}$) was present in the initial test solutions (~ 0.13 mM), indicating that a certain amount of sulfate was already present in the AO 6 solution, due to the impurity. The net $C_{SO_4^{2-}}$ production amounted to 0.43 and 0.46 mM at the end of treatment in the O_3 alone and the O_3/UV experiments, respectively; values agreed with the purity-corrected theoretical sulfate concentrations. In Fig 4(a) and 4(b), within the first 50 min of ozonation, the net $C_{SO_4^{2-}}$ generation rate for the O_3 alone and the O_3/UV systems were 0.68 and 0.8 mM/min, 0.025 and 0.2 mM/min for the time from 50 to 90 min. The results indicated that sulfate groups were easily released from AO 6 molecules under ozone attack and most sulfate was released within the first 50 min. After 50 min, most of AO 6 species were destroyed and formed intermediate products that were persistent with respect to be oxidation in the O_3 alone system. Ozonation with UV irradiation would enhance the removal of intermediates with the release of anionic sulfate. The little difference of net $C_{SO_4^{2-}}$ between the O_3 alone and the O_3/UV system at the end of experiments suggested that UV irradiation on sulfate formation was insignificant under the same ozone dose conditions.

The nitrate concentrations ($C_{NO_3^-}$) were about 0.12 mM in both the O_3 alone and the O_3/UV systems at the end of experiments. The concentration profiles during the cause of oxidation were similar to that of sulfate as described above, only the magnitude was lower. The ammonium ($C_{NH_4^+}$) was found in the initial solution and the extent was less than 0.01 mM; that may due to the impurity existed in target material. The accumulation of $C_{NH_4^+}$ was insignificant (< 0.1 mM) as shown in Fig 4.2a and 4.2b. As comparing with the purity-corrected theoretical nitrogen concentration (0.83 mM), the observed nitrogen concentration (0.22 mM) was about a quarter of its theoretical value. It was found that NO_2, NO, CO_2, and small amount of SO_2 was detected in the off-gas, and the NO_2 concentration reached as high as 170 part per billion at the gas flow rate of 2.1 l/min conditions, suggesting that the low observed nitrogen concentration during the experimental course was because of gaseous nitrogen compounds formed. In fact, some researchers have already reported that organic nitrogen could be oxidized and produced N_2 and NO_x. The wet air oxidation of aniline, showed a distribution of the mineralized by-products of 50% N_2, 40% nitrate and nitrite and 10% NH_4^+ (Oliviero et al., 2003). Photocatalysis of dichlofluanid generated nitrate and NH_4^+ (Sakkas and Albanis, 2003). Photodegradation of direct yellow-12 by using UV/H_2O_2/Fe^{2+} generated CO_2, CO, NO, NO_2, N_2O, SO_2 in a batch system (Rathi et al., 2003).

4.1.4 Ozone consumption associated with DOC removal and anions formation

DOC removal efficiencies (η_{DOC}) for all experiments are shown in Fig. 4.3. At O_3 of 18.7 mg/l-min and in presence of UV irradiation, the η_{DOC} was 100% at about 120 min; whereas η_{DOC} was only 65% and 71% at O_3 of 18.7 and 33.3 mg/l-min, respectively in the O_3 alone system. Further, the ozone dose only affects the rate of

DOC removal, but not the extent of DOC removal. As seen in Fig 4.3, the DOC removal rates were enhanced when color removal at a certain level, indicating that the availability of O_3 molecules for DOC oxidation. Figure 4.4 shows the variation of the mineralization rate, $(DOC_0\text{-}DOC)/t$, with η_{DOC} under various experimental conditions. The results illustrated the effects of ozone dose and UV irradiation on the elimination of DOC. It is seen that UV irradiation does not enhance the mineralization rate significantly when $\eta_{DOC} < 40\%$, but, the effect of ozone dose is remarkable. For the stage of $\eta_{DOC} > 40\%$, the value of $(DOC_0\text{-}DOC)/t$ via O_3/UV were still high while those of the O_3 alone system become low. The intermediates in the later stage of the ozonation of AO 6 such as oxalic acid and formic acid have low reactivity toward ozone molecule (Koch et al., 2002; Cheng et al., 2002). Noting that the value of $(DOC_0\text{-}DOC)/t$ in the early stage of ozonation is low because ozone is consumed mainly for breaking azo bond and opening the aromatic rings. According to the previous studies on the O_3 alone and O_3/UV treatment of Acid Orange 10 (Shu and Huang, 1995) and phenol (Huang and Shu, 1995), the O_3/UV has better performance for the degradation of Acid Orange 10 and phenol than O_3 alone. Thus, the oxidation reaction via •OH radicals is predominant to proceed in the regime with higher η_{DOC}.

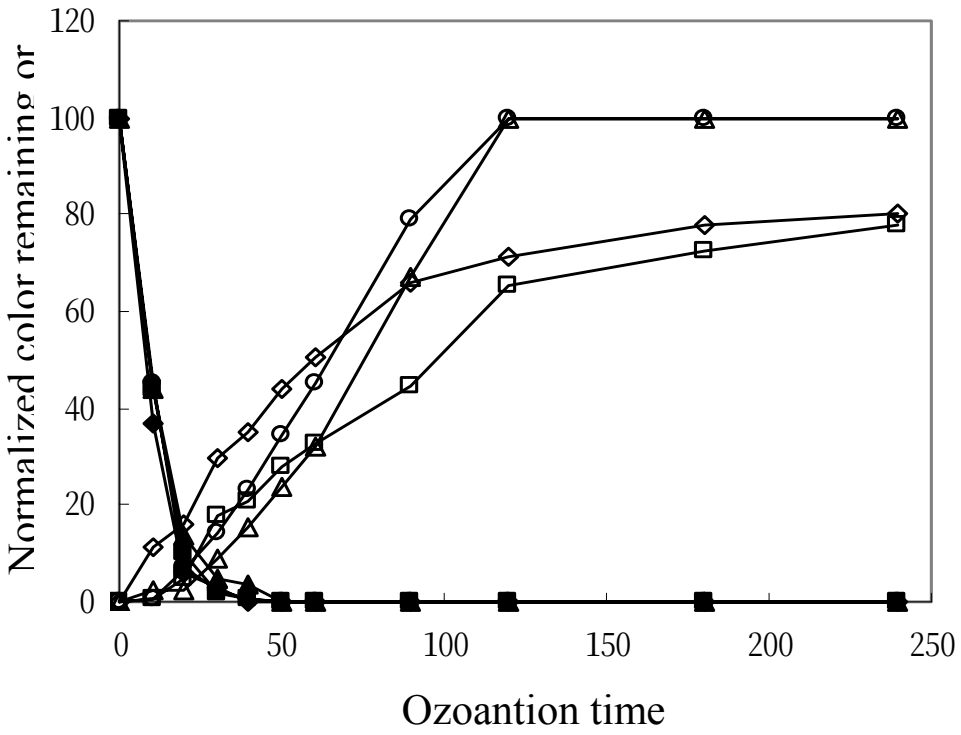

Figure 4.3 The time-course of normalized color remaining (%) and η_{DOC} (%) under different experimental conditions: ■, □: color removal, η_{DOC} at O_3 = 18.7 mg/l-min; ◆, ◇: color removal, η_{DOC} at O_3 = 33.3 mg/l-min; ●, ○: color removal, η_{DOC} at O_3 = 18.7 mg/l-min with UV intensity 15 W/m^2; ▲, △: color removal, η_{DOC} at O_3 = 18.7 mg/l-min with UV intensity 30 W/m^2

The ozone consumption (m_{O_3R}) and ozone applied (m_{O_3A}), eq. 4.1 and 4.2 taken from literature (Chen et al., 2004) were used.

$$m_{O_3R} = \int_0^t Q_G (C_{Ai} - C_{Ae})dt - C_{Al}V_L - C_{Ae}V_H \quad (4.1)$$

$$m_{O_3A} = Q_G C_{Ai} t \quad (4.2)$$

where Q_G as gas feed rate = 2.1 l/min;

C_{Ai} and C_{Ae} as the inlet and outlet O_3 concentration (mg/min);

C_{Al} represented the dissolved O_3 in liquid phase;

V_L as the reaction liquid volume = 5 l;

V_H as the free space in reactor = 0.5 l;

t = reaction time (min).

and the ozone consumption ratio (m_{O3R}/m_{O3A}) was determined as well. The relationship between ozone consumption ratio and η_{DOC} under various experimental conditions were shown in Fig. 4.5, which demonstrated ozone consumption ratio was consistent with DOC removal. Evidently, the ozone consumption ratio for all experimental conditions decreased from 14 to 12% when η_{DOC} < 40% because the decolorization in the early stage of the ozonation of AO 6 might consume relative large amount of ozone. When reaching comple decolorization, the ozone consumption ratio will decrease to a constant level. It is noted that the ozone consumption ratio at high ozone dose (33.3 mg/l-min) decreased rapidly when η_{DOC} > 50%, suggesting that the amount of consumed ozone decreased as persistent by-products formed. As seen in Fig. 4.5, the ozone consumption ratios of the O_3/UV system were slightly higher than that of the O_3 alone system, indicating that UV irradiation will catalyze the ozone decomposition (Hautaniemi et al., 1998).

Figure 4.6 illustrates the relationship between sulfate and nitrate generation ozone consumption. It is noted that UV irradiation slightly enhance the amount of

sulfate generation when m_{O3R} < 20 mmole, as shown in Fig 4.6a. For the stage of m_{O3R} > 20 mmole, the sulfate generation amount via O_3/UV was slightly higher than those of the O_3 alone system. For nitrate formation, as shown in Fig 4.6(b), the enhancement of UV irradiation is not as significant as sulfate, but, the effect of ozone dose was remarkable. It is suggested that more sulfate is formed at early stage of ozonation than nitrate, proving that sulfate is easier to be released from AO 6 molecule than nitrate.

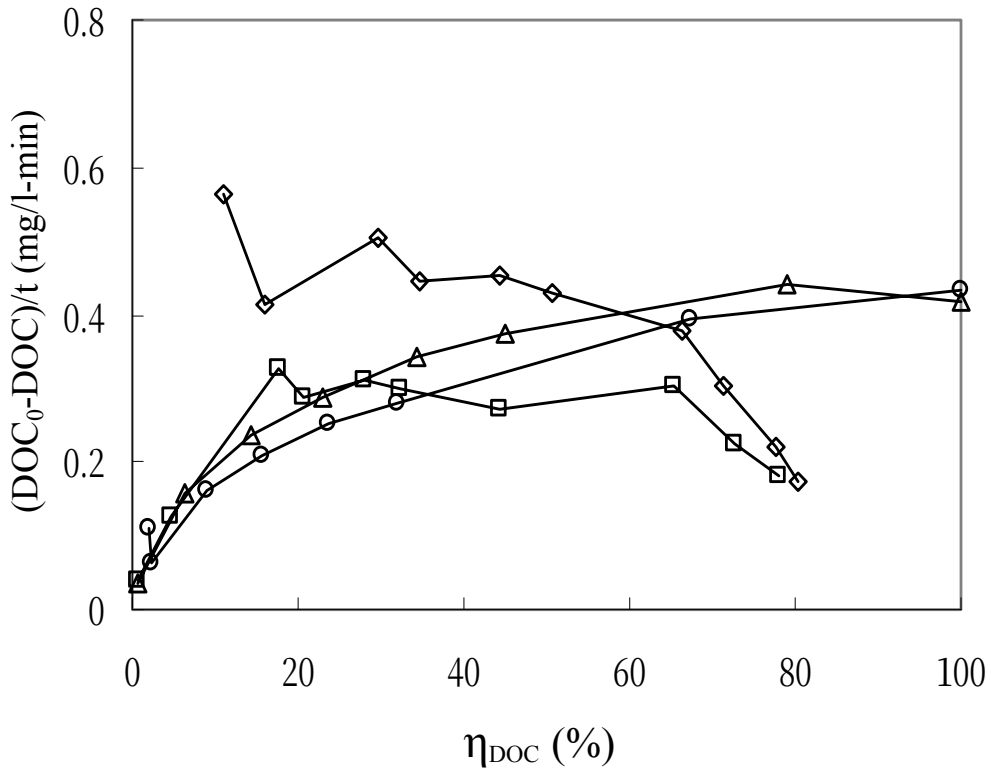

Figure 4.4 $(DOC_0\text{-}DOC)/t$ vs. η_{DOC} (%)under different experimental conditions: □: O_3 = 18.7 mg/l-min, ◇: O_3 = 33.3 mg/l-min, ○: O_3/UV at O_3 = 18.7 mg/l-min with UV intensity 15 W/m^2, △: O_3/UV at O_3 = 18.7 mg/l-min with UV intensity 30 W/m^2.

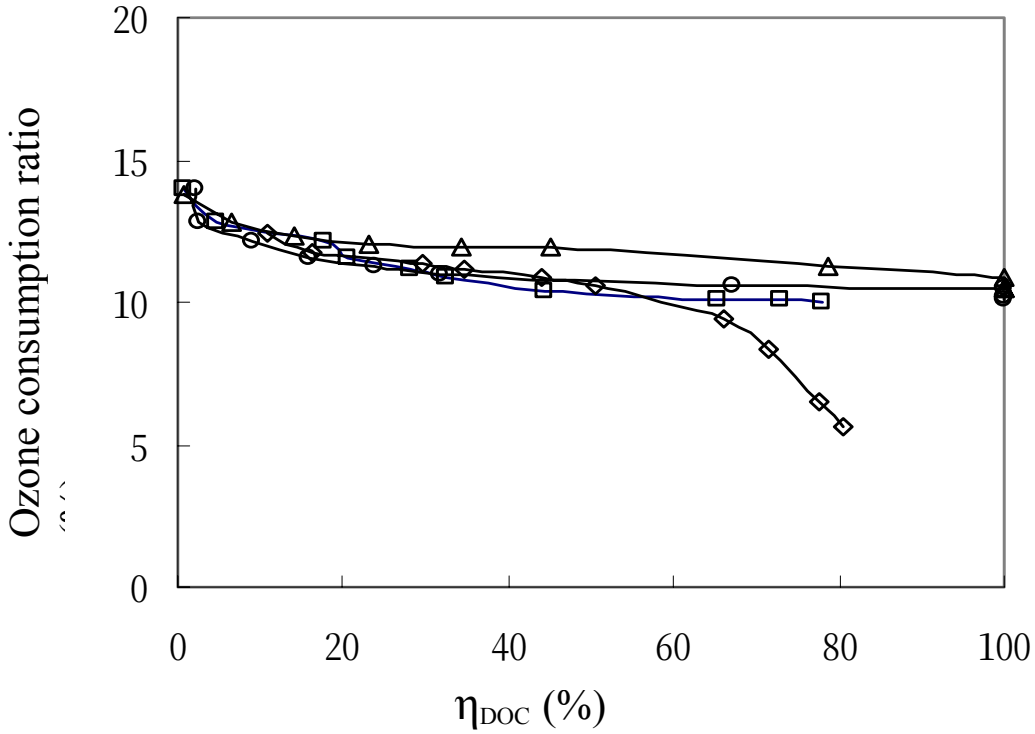

Figure 4.5 Ozone consumption ratio (%) vs. η_{DOC} (%) under different experimental conditions. Notation: □: O_3 = 18.7 mg/l-min, ◇: O_3 = 33.3 mg/l-min, ○: O_3/UV at O_3 = 18.7 mg/l-min with UV intensity 15 W/m^2, △: O_3/UV at O_3 = 18.7 mg/l-min with UV intensity 30 W/m^2.

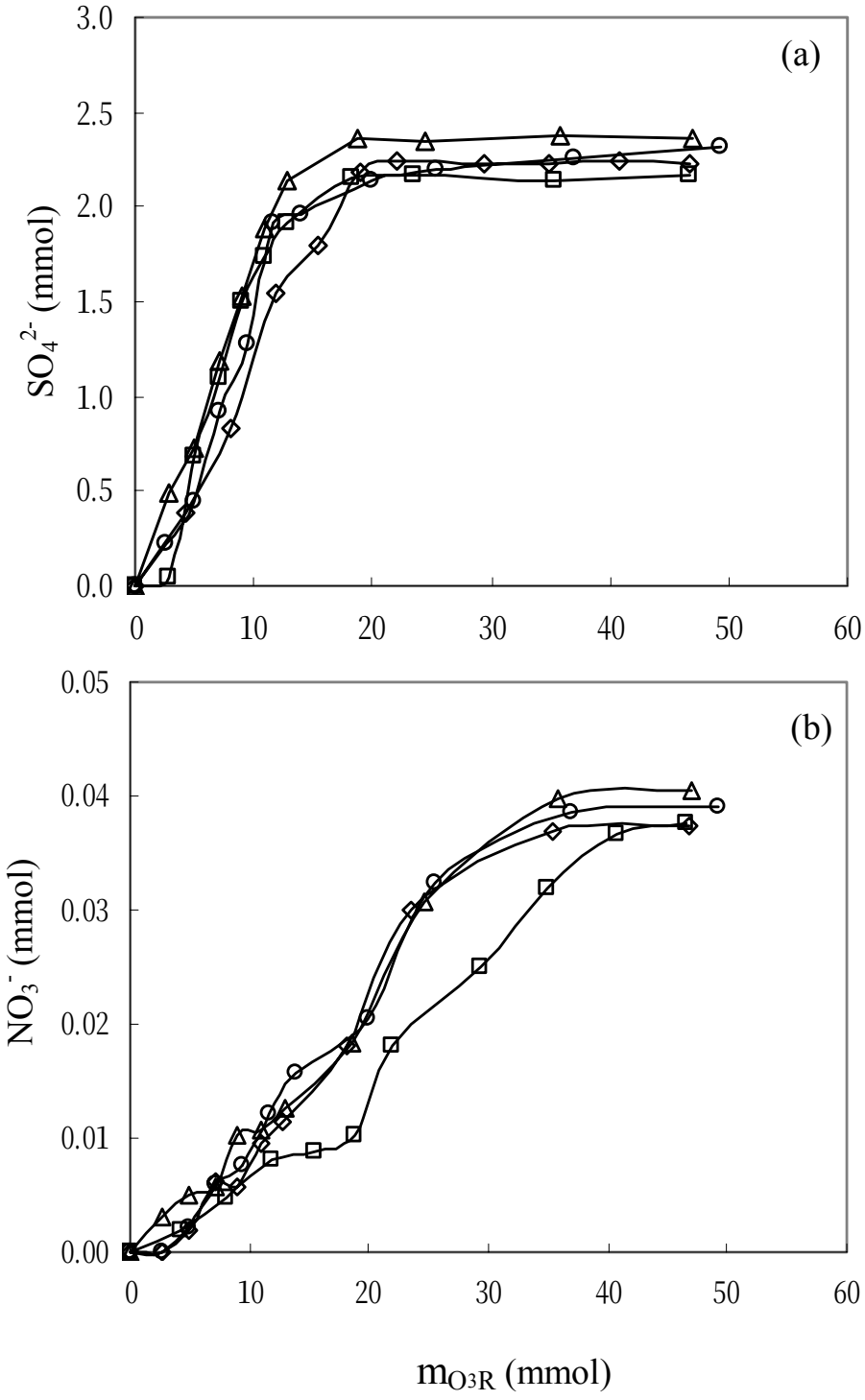

Figure 4.6 The variation of (a) SO_4^{2-} and (b) NO_3^- vs. m_{O3R} under different experimental conditions. Notation: □: O_3 = 18.7 mg/l-min, ◇: O_3 = 33.3 mg/l-min, ○: O_3/UV at O_3 = 18.7 mg/l-min with UV intensity 15 W/m^2, △: O_3/UV at O_3 = 18.7 mg/l-min with UV intensity 30 W/m^2.

4.1.5 The controlling factor effects on AO 6 reduction, decolorization, and TOC removal

1. Temperature

The AO 6 reduction exhibited an exponential decay trend which was similar to the decolorization of azo dye. Both reactions have been considered as a first order reaction (Langlais and Reckhow, 1990). With sufficient ozone, the decolorization reaction of AO 6 can be described by a pseudo first-order reaction equation that has been reported elsewhere (Wu and Wang, 1998; Hao et al, 2000). As noted in the Arrhenius equation, the reaction rate of a given chemical reaction is increased with raising temperatures. This relationship was verified in this study and is shown in Fig. 4.7a. In Fig. 4.7a, as temperature increased, the AO 6 reduction, decolorization, and TOC removal also increased. The k for AO 6 reduction increased from 0.10 ~ 0.20 min^{-1} as temperature raised from 15 to 35 ^{o}C, the determined coefficient (R^2) was 0.98; for decolorization k increased from 0.14 ~ 0.17 min^{-1} and R^2 was 0.98; for the k values of TOC removal, it increased from 0.016 to 0.029 min^{-1} and R^2 was 0.94.

The results revealed that the k values of AO 6 reduction, decolorization, and TOC removal were affected by the rising temperature. The temperature effect on TOC removal was more significant than on decolorization, the increment percentage of the k values for TOC removal was 35% as temperature raised from 15 to 35 ^{o}C, the increment for decolorization k was about 21%.

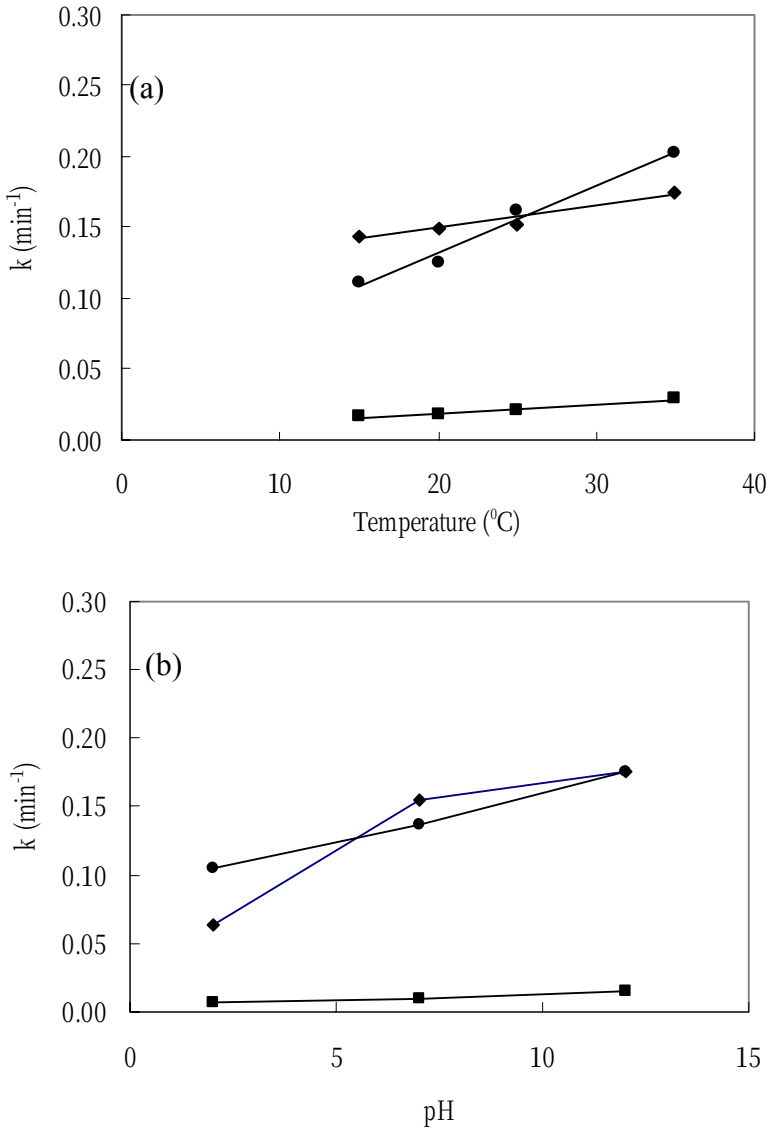

Figure 4.7 The Effects of (a) Temperature and (b) pH on the Decolorization and Removals of AO6 and TOC. Symbol: ●: AO 6, ■: TOC removal, ◆: Decolorization.

2. pH change

Fig. 4.7b illustrates the effects of pH value on the k values of AO reduction, decolorization, and TOC removal. The results indicated that AO reduction, decolorization, and TOC removal rate constants were pH dependent. As pH varied from 2 to 12, the k values for AO 6 reduction, decoloriztion and TOC removal were enhanced with the increase of pH. This experiment was conducted under the following conditions: [AO 6] = 200 mg/l, ozone dose = 2.9 mg/l-min, and temperature at 25 ^{o}C. As mentioned in the previous section ozonation in water could be divided into direct and indirect reactions depending on pH (Rice, 1997). Under indirect ozone reaction, ozone dissolved into aqueous solution and hydroxyl free radical (OH•) was formed. It was reported that at a higher pH value with more OH•, indirect ozone reaction is prevailing (Langlais et al 1991). In this study, it was found that the k values for AO reduction, decoloriztion, and TOC removal were higher at high pH conditions than that in low pH conditions. Findings from this study regarding the effect of hydroxyl free radicals confirm reports from previous investigators. Because of the nature of OH•, the declorization processes became faster as more OH• radicals were generated and attacked on N=N, that would cause the chromophores to detach from aromatic rings. At pH value higher than 7, no dissolved ozone was observed during experimental runs and indicated that indirect ozone reaction was dominated and OH• were generated.

3. Ozone dose

It was reported that the AO6 decolorization process was strongly affected by the ozone dose and the chromophoric structures of dyes reacted rapidly with ozone and OH• (Adams and Gorg, 2002). The effect of ozone dose on the k for AO6 reduction was significant and the results are shown in Fig. 4.8. As the ozone dose increased

from 2.7 to 3.5 mg/l-min, the k for AO 6 reduction increased from 0.13 to 0.22 min^{-1} and the k for decolorization increased from 0.14 to 0.27 min^{-1}. Both rate increases were more than 69%. The significant increase in k suggests that ozone dose plays an important role in AO 6 reduction and decolorization. It also was observed in this study that the k values were higher under basic conditions where OH ions are predominant. The chromophoric structures and azo bonds of AO6 were attacked by ozone and OH• resulting in higher k values. The effect of ozonation on TOC removal was not as significant as that on AO 6 reduction and decolorization. The k value of TOC removal was increased only by approximately 20%. It revealed that decolorization was more vulnerable by the affect of ozone dose than TOC. Clearly, it needs more dissolved ozone molecules and OH· to reduced TOC than that uses in breaking N=N bonding. As a result, decolorization showed a significant linear trend with ozone dose.

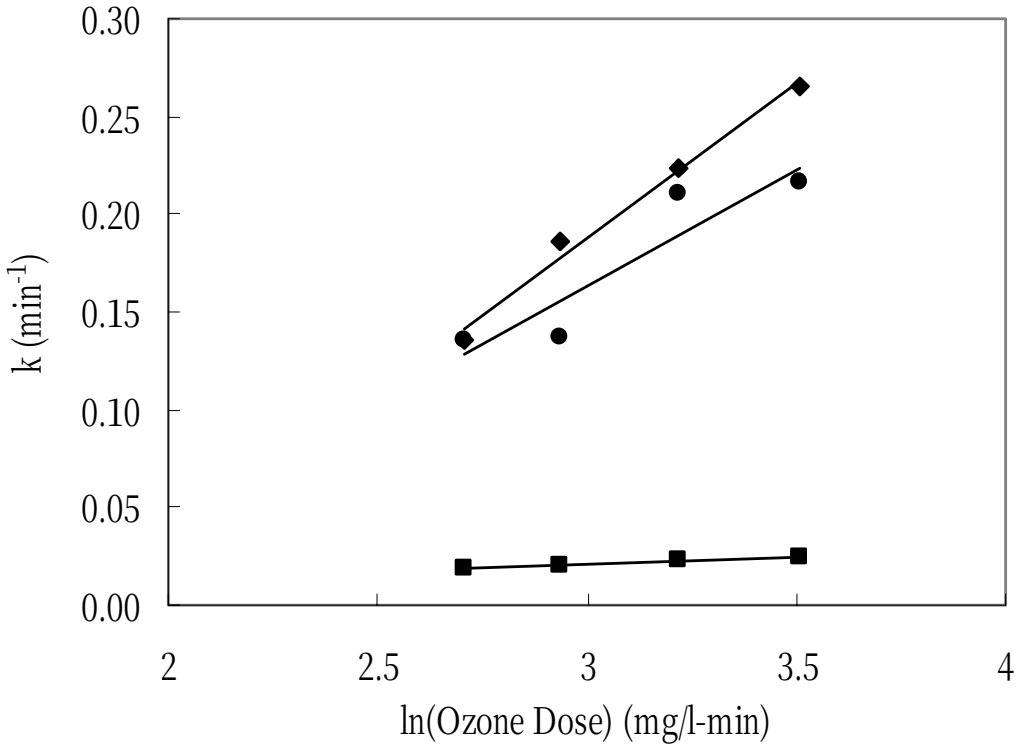

Figure 4.8 The effect of ozone dose on the decolorization and TOC removal. Symbol: ●: AO 6, ■: TOC removal, ◆: Decolorization.

4. **TOC removal associated with sulfate formation**

As mentioned, sulfate formation was proportionally increased with TOC removal efficiency (η_{TOC}). In the ozonation process, aromatic rings of AO6 were opened and the TOC was oxidized to carbon dioxide. In this process, sulfate was released and the amount of sulfate would increase as the process continued. The relationship between sulfate yield ($Y_{SO_4^{2-}}$), decolorization and η_{TOC} was investigated and the results are shown in Fig. 5, where:

$$Y_{SO_4^{2-}} = \Delta C_{SO_4^{2-}} / C_{AO6} \quad (4.3)$$

$$\eta_{TOC} = 1 - C_{TOC} / C_{TOC_0} \quad (4.4)$$

The decolorization proceeded quickly when η_{TOC} increasing, indicating that TOC removal accompanied with decolorization, nonetheless, the $Y_{SO_4^{2-}}$ increased too. When η_{TOC} > 0.4, the decolorization almost was completed and the increment of $Y_{SO_4^{2-}}$ was accelerated, indicating that most ozone or OH• were attacking TOC after the completion of the decolorization process. From Fig. 4.9, it is observed that the temperature effect on $Y_{SO_4^{2-}}$ values was significant when the $Y_{SO_4^{2-}}$ values ranged from 0.31 to 0.96.

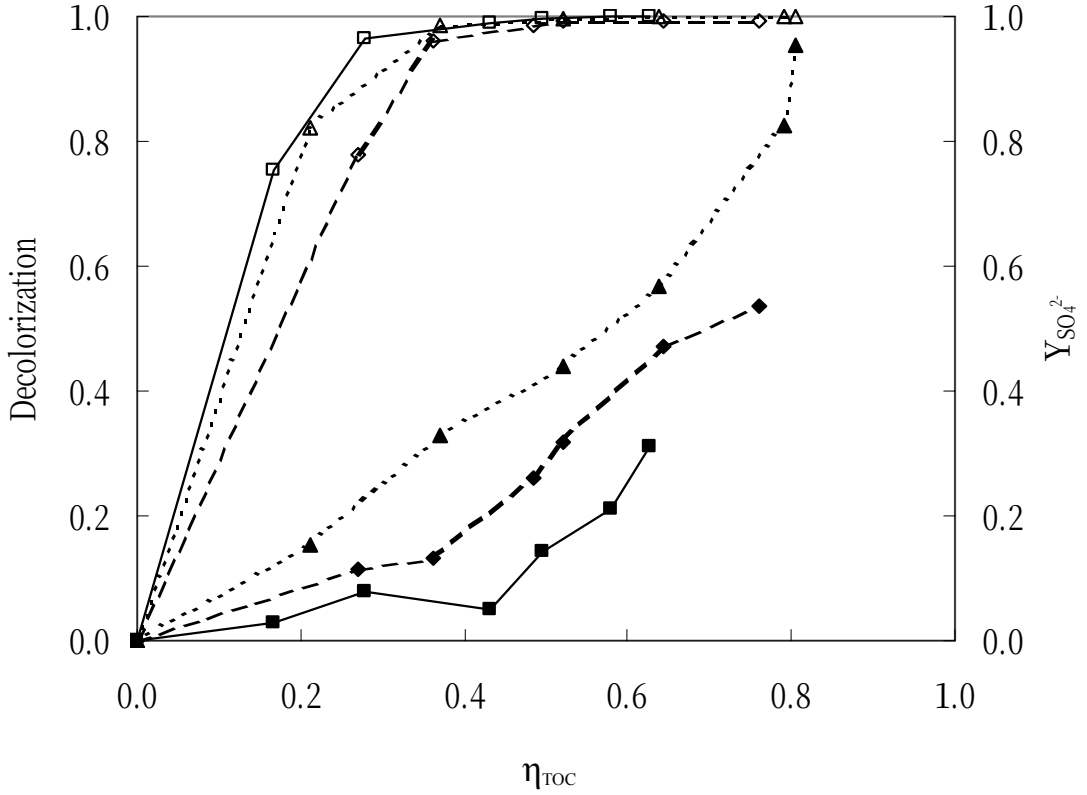

Figure 4.9 The variation of $Y_{SO_4^{2-}}$ and color remaining vs. TOC removal efficiency under 15, 25, and 35 ℃ with pH = 7, [AO 6] = 200 mg/l, ozone dose = 9 mg/l/min. Symbol: $Y_{SO_4^{2-}}$ and color, ■ and □ : 15 °C; ◆ and ◇ : 25 °C; ▲ and △ : 35 °C.

5. Toxicity assessment for selected ozonation processes

The toxicity assessment was conducted in this study that used Microtox reagent as an indicator by measuring the luminescent of photobacteria in cells. The toxicity for the samples collected at different reaction time (0, 1, 2, 3, 5, 10, and 20 min) was evaluated and the results were shown in Fig. 4.10. The results showed that AO 6 did inhibit the incubated cultures initially, than, after 30 min of ozone and/or O_3/UV treatment, the effect of inhibition on the luminescent of incubated cultures disappeared. The initial 15 min-EC50 value for O_3 alone and the O_3/UV was 23.48%; as reaction time = 10 min, the 15 min-EC50 value increased to 100% for the sample treated by O_3/UV, but 15 min-EC50 value for the sample of O_3 alone was only 49%. The results indicated that initial AO 6 solution was toxic, after treated by O_3 alone and the O_3/UV, the toxic reduction of AO 6 was observed clearly. However, as decolorization approaching to 100%, the 15 min-EC50 values reached to 100%, indicating that the ozonated by-products were not toxic. The results suggested that O_3 alone and the O_3/UV could enhance the decolorization, mineralization and toxic reduction of AO 6.

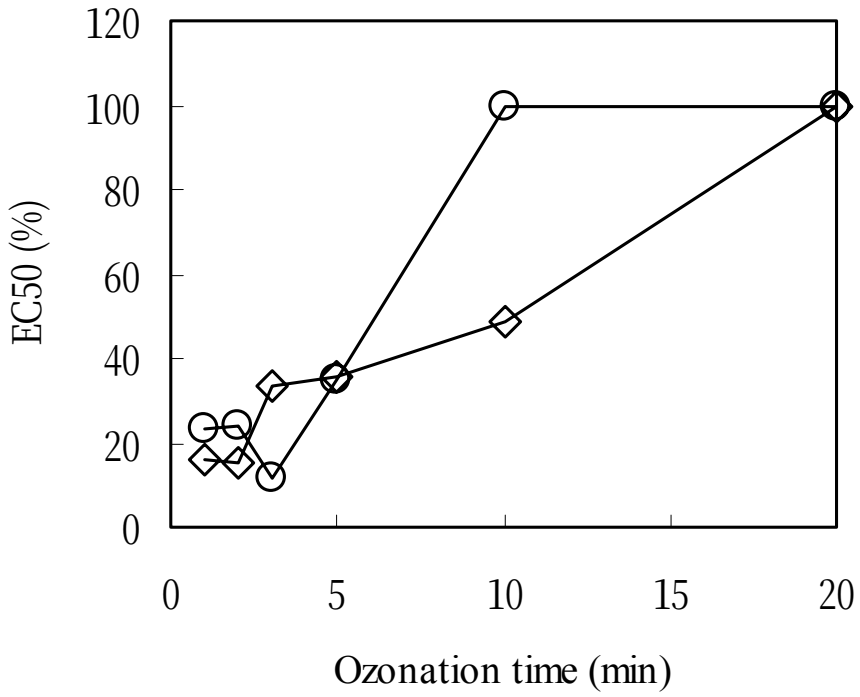

Figure 4.10 Variation of EC50 (%) under O_3 = 18.7 mg/l-min (□) and O_3 = 18.7 mg/l-min with UV intensity 30 W/m^2 (○)

4.2 The reaction kinetics prediction of AO 6 by ozone

1. The Development of Simplified Multi-step Reaction Kinetic Model

The assumptions of the Multi-step Reaction Kinetic Model (MSRK) model in the semi-continuous ozonation condition is adopted from Chen (2004), the similar assumption are used that are as follows.

1. The homogeneous conditions with complete mixing of liquid and gas flows are valid in the reactor.
2. Series ozonation mechanism is applicable.
3. Second-order chemical reactions are bimolecular.
4. Henry's law applies.
5. Reactions in the gas phase are neglected.

For the governing equation of holdup gas ozone (C_{AGi}) can be expressed by eq 4.5.

$$dC_{AGi}/dt = Q_G(C_{AGi0} - C_{AGi})/V_H - k^0_{LA}\,a(C_{AGi}/H_A - C_{ALb})/\varepsilon_G \quad (4.5)$$

For the governing equations of dissovled ozone (C_{ALb}), C_{BLb} and intermediates (C_{jLb}) in the liquid phase, the chemical reaction terms should be expressed as eq 4.6–4.9.

For C_{ALb},

$$dC_{ALb}/dt = k^0_{LA}\,a(C_{AGi}/H_A - C_{ALb})/\varepsilon_L - k_dC_{ALb} - k_BC_{ALb}C_{BLb} - \Sigma\, k_j\, C_{ALb}C_{jLb} \quad (4.6)$$

For C_{BLb},

$$dC_{BLb}/dt = -k_BC_{ALb}C_{BLb} \quad (4.7)$$

For C_{jLb}

$$dC_{jLb}/dt = k_{j-1}C_{ALb}C_{j-1Lb} - k_jC_{ALb}C_{jLb} \quad (4.8)$$

The concentration of ozonated product (C_{PLb}), which has relatively low reactivity toward ozone, is calculated by eq 4.9

$$C_{PLb} = C_{BLb0} - C_{BLb} - \Sigma C_{jLb} \quad (4.9)$$

The governing equation of off-gas ozone (C_{AGe}) in the free space (Andreozzi et al., 1991) is:

$$dC_{AGe}/dt = Q_G (C_{AGi} - C_{AGe})/V_F \quad (4.10)$$

where V_F = volume of free space. The initial conditions of eqs 1–6 are:

$$t = 0, C_{AGi} = C_{AGe} = C_{ALb} = C_{jLb} = C_{PLb} = 0, C_{BLb} = C_{BLb0} \quad (4.11)$$

The variation of TOC can be estimated by eq 4.12:

$$C_{TOC}/C_{TOC0} = (C_{BLb} + \Sigma \alpha_j C_{jLb} + \alpha_p C_{PLb})/C_{BLb0} \quad (4.12)$$

where

a	= specific gas-liquid interfacial area based on the volume of liquid and gas
C_{AGi}, C_{AGi0}	= gas concentrations of ozone of holdup and inlet gases
C_{AGe}	= gas concentration of ozone in free volume
C_{ALb}	= dissolved ozone concentrations in bulk liquid
C_{BLb}	= concentration of pollutant in bulk liquid
C_{BLb0}	= initial concentration of pollutant in bulk liquid
C_{PLb}	= concentration of ozonated product
C_e, $\overline{C_e}$	= experimental data and the corresponding average values
C_{jLb}	= concentration of intermediate j in bulk liquid
C_p	= predicted values
C_{TOC}	= concentration of total organic carbons
C_{TOC0}	= initial concentration of total organic carbons
H_A	= dimensionless Henry's law constant of ozone, C_{AGi}/C_{ALS}, $He/(R_G T)$
He	= Henry's law constant of ozone, p_{Ai}/C_{ALS}
I_j	= intermediate j
j	= intermediate j, Arabic numbers
k_B	= ozonation rate constant of pollutant B
$k_{B,App}$	= apparent ozonation rate constant of pollutant B

k_d = self-decomposition rate constant of ozone

k_j = ozonation rate constant of intermediate j

k_L^0 = physical liquid-phase mass transfer coefficient

k_{LA}^0 = physical liquid-phase mass transfer coefficient of ozone, m/s

k_{LO}^0 = physical liquid-phase mass transfer coefficient of oxygen, m/s

R^2 = determination coefficient, $1 - [\Sigma (C_e - C_p)^2 / \Sigma (C_e - \overline{C_e})^2]$

Q_G = gas flow rate

V_F = volume of free space

V_H = volume of holdup gas

V_L = volume of bulk liquid

α_j, α_p = ratios of TOC contributions per mole of intermediate j and of product P to that per mole of pollutant B

ε_G, ε_L = relative gas and liquid holdups, $\varepsilon_G + \varepsilon_L = 1$

θ_{TOC} = dimensionless TOCs concentration, C_{TOC}/C_{TOC0}

θ_{AGe} = dimensionless gas concentration of ozone in free volume

θ_{ALb} = dimensionless concentration of ozone in bulk liquid

θ_{BLb} = dimensionless concentration of pollutant in bulk liquid

The actual reactions between ozone and pollutants may be more complex than the proposed multi-step reactions with these simplifying assumptions as forementioned. However, the present reactions kinetic model provides a simplified explanation of the experimental data for practical engineering application. Thus, the validity of the model must be justified by comparing the agreeability of model and experimental results as examined in the latter sections.

2. The determination of parameters used

The fraction of ε_G is calculated by the volume-expanding method employing $\varepsilon_G = V_H/(V_H + V_L)$ that is 0.023 for AO 6 solution and 0.017 for aqueous solutions, respectively. The average d_{bs} is about 0.729 mm by measuring the bubble images and the specific area of gas-liquid interface (a) can be calculated with $a = 6\varepsilon_G/d_{bs}$, the

dimensionless H_A is 4.18 MM^{-1} (Chen et al., 2004). The volumetric mass transfer coefficient of oxygen ($k^0_{LO}a$) in the aqueous solution is measured as 0.0268 s^{-1} by oxygen aeration. The diffusion coefficients of oxygen (D_O) and ozone (D_A) in the AO 6 solution are estimated according Wilke and Chang (1955). The values of k^0_{LO} and k^0_{LA} can be estimated by using surface renew theory (k^0_L å $D^{0.5}$) that are 1.28×10^{-4} and 1.15×10^{-4} m s^{-1}. The k_d can be estimated as 1.45×10^{-4} s^{-1} by using the formula proposed by Gurol and Singer (1982).

The variations of C_{BLb}, C_{TOC}, C_{ALb} and C_{AGe} are simultaneously monitored for the purpose of MSRK model verification. The normalized concentrations in the dimensionless forms of C_{BLb}, C_{TOC}, C_{ALb} and C_{AGe} are: θ_{BLb} (= C_{BLb}/C_{BLb0}), θ_{ALb} (= $C_{ALb}/(C_{AGi0}/H_A)$), θ_{AGe} (= C_{AGe}/C_{AGi0}), and θ_{TOC} (= C_{TOC}/C_{TOC0}).

3. Simulation of AO 6's Ozonation

Appropriated kinetic parameters can be obtained by achieving the best fitting for the experimental data in the simulation with MSRK models with various steps of reactions, and the corresponding values of the parameters and determination coefficient (R^2) are summarized in Table 1. As the number of reaction step ascending, the R^2 values get improving, suggesting that adopting higher step of reaction kinetic model may well predict the variation of C_{BLb}, C_{TOC}, C_{ALb} and C_{AGe}. The variation of dimensionless parameters, θ_{ALb}, θ_{AGe}, θ_{BLb}, and θ_{TOC}, are predicted and verified with experimental data. It is clearly that higher reaction steps of the kinetic model would enhance the R^2 value of data fitting, the results indicating that the five-step reaction can well express the reaction kinetics simulation. Furthermore, five-step reaction may indicate four intermediates that are produced during ozonation.

As azo bond (N=N) attacking by ozone, the AO 6 molecules and color disappear rapidly that are measured in all experiments. It indicates that the reaction rate constant of AO 6 with ozone (k_1 = 120000 $M^{-1}s^{-1}$) is considerably high due to high reactivity of N=N, and the decolorization reaction will be faster than the breakage of

aromatic rings. The TOC contribution of the intermediate I_j is reflected by the factor α_j with smaller value of α_j indicating higher mineralization degree or lower value of C_{TOC}/C_{TOC0} as revealed by eq 4.12. Based on the predict α_1 (= 1.0) value, none of the organic carbon of AO 6 is oxidized to CO_2 in the initial reaction, indicating that result may support the decolorization happened prior to TOC reduction.

Table 4.1. Ozonation Kinetics of AO 6 Adopting Schemes with Various Reaction Steps

Reaction step	Kinetic parameter	R^2 value for predicted results			
		θ_{BLb}	θ_{TOC}	θ_{ALb}	θ_{AGe}
2	$k_1 = 120000\ M^{-1}s^{-1}$, $k_2 = 1.5\ M^{-1}s^{-1}$	0.877	0.918	< 0.1	0.975
3	$k_1 = 120000\ M^{-1}s^{-1}$, $k_2 = 24000\ M^{-1}s^{-1}$, $k_3 = 1.55\ M^{-1}s^{-1}$	0.90	0.939	< 0.1	0.980
4	$k_1 = 120000\ M^{-1}s^{-1}$, $k_2 = 24000\ M^{-1}s^{-1}$, $k_3 = 3500\ M^{-1}s^{-1}$, $k_4 = 1.55\ M^{-1}s^{-1}$	0.973	0.961	0.680	0.983
5	$k_1 = 120000\ M^{-1}s^{-1}$, $k_2 = 24000\ M^{-1}s^{-1}$, $k_3 = 3500\ M^{-1}s^{-1}$, $k_4 = 10\ M^{-1}s^{-1}$, $k_5 = 1.55\ M^{-1}s^{-1}$	0.979	0.989	0.756	0.984

4. The variations of θ_{BLb}, θ_{TOC}, θ_{ALb}, and θ_{AGe}

It is known that the removal amount of target compound is concerned with fed ozone concentration (C_{AGi0}). The higher C_{AGi0} provided, the less θ_{BLb} will be achieved, as shown in Fig. 4.11. The times required for the complete removal of AO 6 with C_{AGi0} = 6 mg/L/min (30min) is about 6, 3, and 1.2 times of those with C_{AGi0} = 16 (5 min), 12 (10 min), and 9 mg/L/min (25 min), respectively. The pseudo-first-order reaction rate expression can be proposed as $\theta_{BLb} = \exp^{-k_{B,App}}$ with $k_{B,App} = 0.0934\ C_{AGi0}\ min^{-1}$ (where C_{AGi0} in mg/L) from the experimental data.

Again, the variation of TOC reduction may be observed by changing the C_{AGi0} value, as shown in Fig. 4.12, which illustrates the variation of $\boldsymbol{\theta_{TOC}}$ under different experimental conditions. It is clearly that the C_{AGi0} value can accelerate the mineralization rate correspondingly, the same as observed in θ_{BLb}. As seen in Fig. 4.12, it is observed that the variation of θ_{TOC} can be divided into two segments, as θ_{TOC} about 0.8 as the turning point. As in the case of C_{AGi0} = 16 mg/L/min, the value of $\Delta\theta_{TOC}/\Delta t$ is 0.039 for the reaction from 0 to 20 min and 0.0059 for the time from 20 to 60 min, indicating that the slow progress of the mineralization is happened after reaction time = 20 min.

As shown in Fig 4.13, the variations of θ_{ALb} can be divided into three stages. In the case of C_{AGi0} = 16 mg/L/min, in the first stage (with $\theta_{TOC} > 0.9$), the θ_{ALb} almost undetectable and the variation of θ_{BLb} is very fast (Fig. 4.11), indicating that the ozone transferred from the gas phase is consumed immediately in the solution by breaking the azo bonds mostly. As decolorization completed, the θ_{ALb} starts to increase rapidly with ozonation time in the transient regime (with $0.77 \leq \theta_{TOC} < 0.97$), suggesting that the amount of dissolved ozone accumulation is larger than that of the consumption. The result may due to the generation of refractory intermediates which reactivity is far lower than the target compound. In the final stage, the θ_{ALb} approaches to the constant value of about 0.5 and is independent of C_{AGi0}.

The ozone concentration in the off-gas is monitored in this study and the results are shown in Fig. 4.14. The θ_{AGe} increases consistently from the beginning to reach the steady state; it is corresponding to the θ_{BLb} decreasing. The results suggest that the amount of θ_{ALb} is consumed in the ways of self-decomposition and chemical reaction in early stage of ozonation, the θ_{AGe} will increase as reaction time increasing that is due to the dissolved ozone for reaction need decreasing. As C_{AGi0} increasing,

the more unused ozone appears in off-gas, the amount is higher than that for the need of dissolves into liquid phase, self-decomposition, and chemical reaction, indicating that the ratio of ozone transferred from gas to liquid phases to that in feed gas decreases with ozonation time.

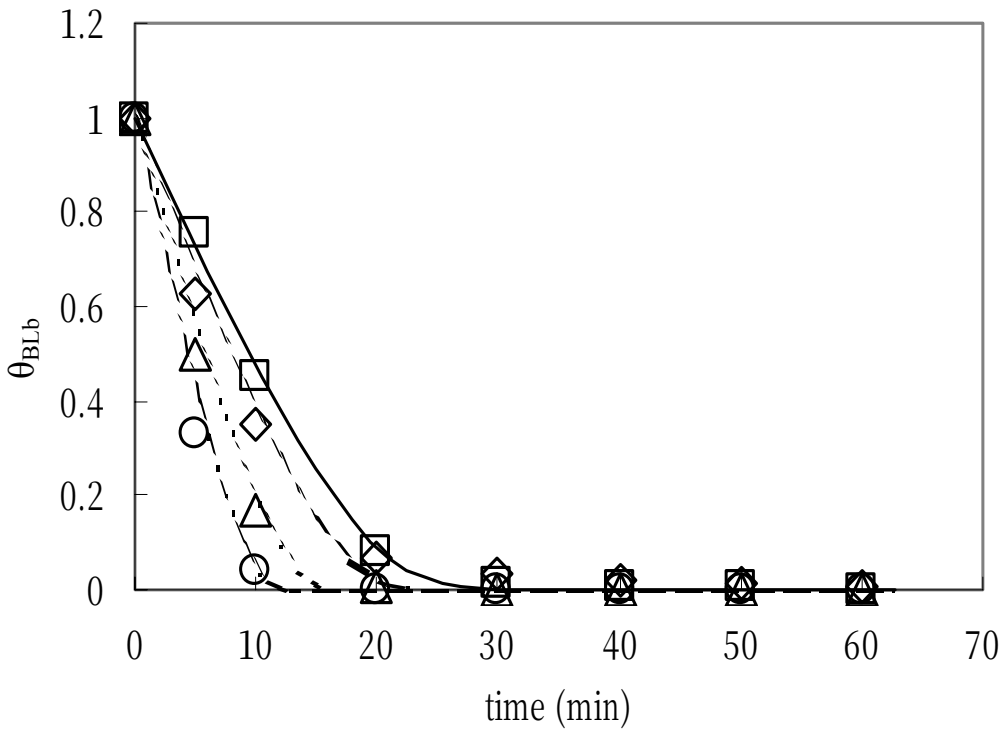

Figure 4.11. Time variations of θ_{BLb} for AO 6 ozonation in a semibatch system. $\theta_{BLb} = C_{BLb}/C_{BLb0}$. Symbols: experiments; lines: prediction based on five-step reaction kinetics. _ _ _ □ and —— : C_{AGi0} = 6 mg/L/min. _ . _ ◇ and : C_{AGi0} = 9 mg/L/min. △ and : C_{AGi0} = 12 mg/L/min. ○ and : C_{AGi0} = 16 mg/L/min.

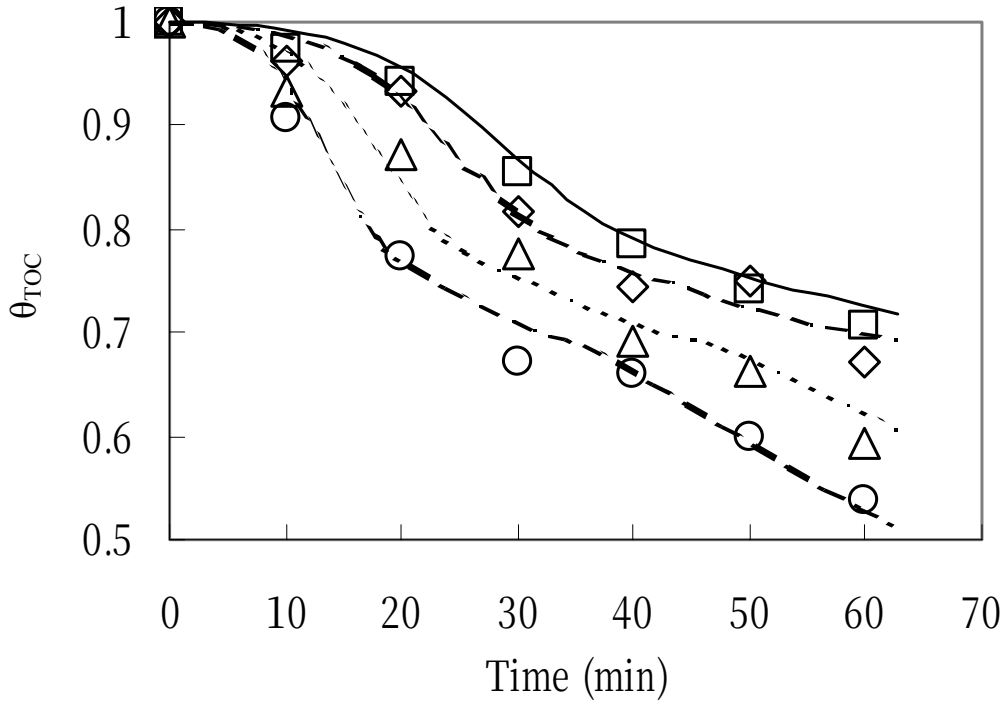

Figure 4.12 Time variations of θ_{TOC} for AO 6 ozonation in semibatch system. $\theta_{TOC} = C_{TOC}/C_{TOC0}$. Symbols: experiments; lines: prediction based on five-step reaction kinetics. Symbols: experiments; lines: prediction based on five-step reaction kinetics. □ and —— : C_{AGi0} = 6 mg/L/min. ◇ and : C_{AGi0} = 9 mg/L/min. △ and : C_{AGi0} = 12 mg/L/min. ○ and : C_{AGi0} = 16 mg/L/min.

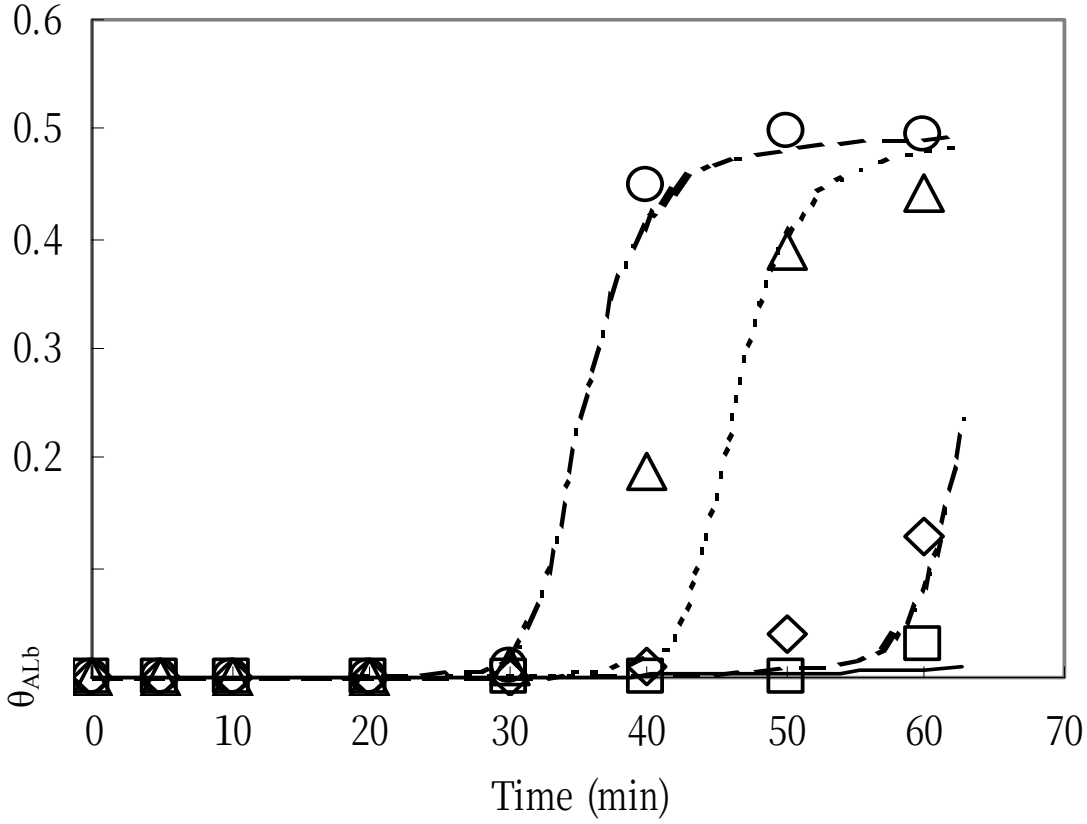

Figure 4.13 Time variations of θ_{ALb} for AO 6 ozonation in semibatch system. $\theta_{ALb} = C_{ALb}/(C_{AGi0}/H_A)$. Symbols: experiments; lines: prediction based on five-step reaction kinetics. Symbols: experiments; lines: prediction based on five-step reaction kinetics. □ and —— : C_{AGi0} = 6 mg/L/min. ◇ and : C_{AGi0} = 9 mg/L/min. △ and : C_{AGi0} = 12 mg/L/min. ○ and : C_{AGi0} = 16 mg/L/min.

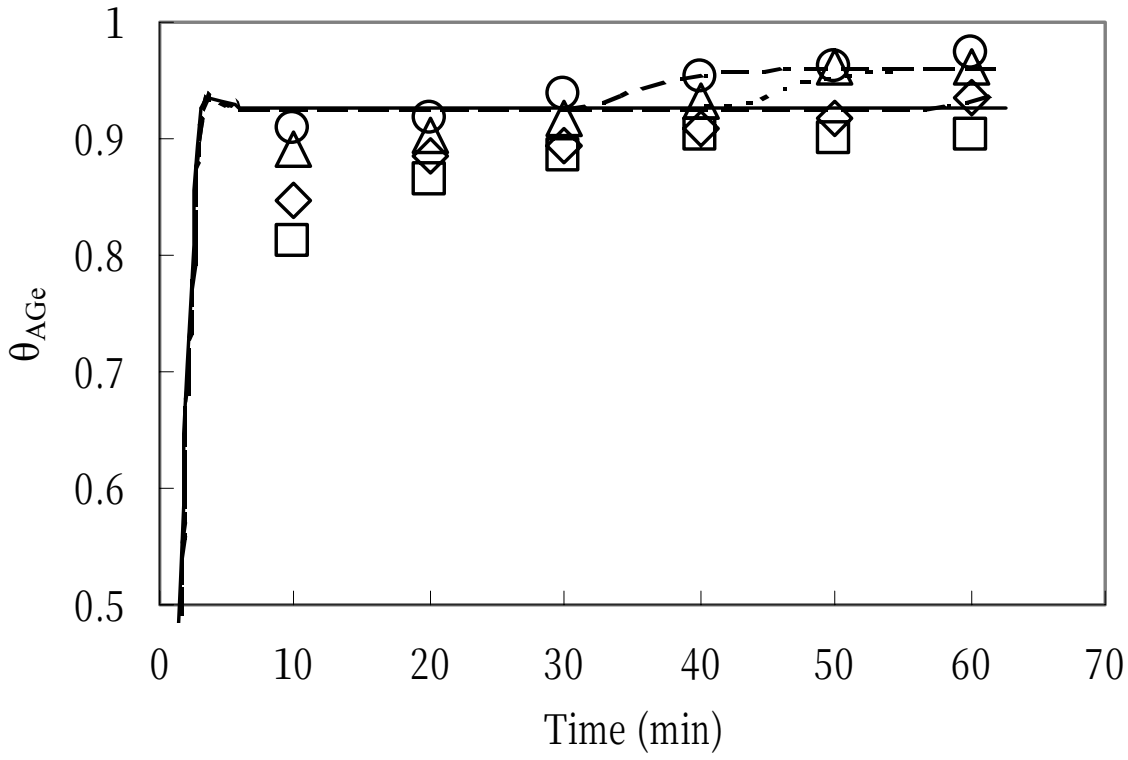

Figure 4.14 Time variations of θ_{AGe} for AO 6 ozonation in semibatch system. $\theta_{AGe} = C_{AGe}/C_{AGi0}$. Symbols: experiments; lines: prediction based on five-step reaction kinetics. Symbols: experiments; lines: prediction based on five-step reaction kinetics. □ and —— : C_{AGi0} = 6 mg/L/min. ◇ and : C_{AGi0} = 9 mg/L/min. △ and : C_{AGi0} = 12 mg/L/min. ○ and : C_{AGi0} = 16 mg/L/min.

4.3 Bubble column system

4.3.1 Tracer test

In order to testify the design feasibility of bubble column, following tracer tests are conducted under different flow conditions, i.e. liquid flow = 10, 12, 14 L/min and gas flow = 0.9, 2.1, 2.7 L/min respectively, that was the large flow rate patterns. For the small flow rate patterns, the liquid flow = 2, 2.4, 2.7, 3.2, 4, and 6 L/min and gas flow = 0.9, 2.1, 2.7, and 3.2 L/min respectively. The tracer test results for large and small flow rate patterns were shown as Table 4.2 and 4.3. The monitoring results of tracer flowed out from bubble column were shown as Fig. 4.10.

Based on the report written by Levenspiel (1972), the residence time distribution (RTD) may relate to the mean residence time (MRT), denoted as $\bar{t}$, and $\bar{t}$ can be expressed as follows:

$$\bar{t} = \frac{\int_0^\infty tCdt}{\int_0^\infty Cdt} = \frac{\sum t_i C_i \Delta t_i}{\sum C_i \Delta t_i}, \tag{4.13}$$

and the variance (σ^2)can illustrate as following form

$$\sigma^2 = \frac{\int_0^\infty (t-\bar{t})^2 Cdt}{\int_0^\infty Cdt} = \frac{\int_0^\infty t^2 Cdt}{\int_0^\infty Cdt} - \bar{t}^2, \tag{4.14}$$

or in discrete form,

$$\sigma^2 \cong \frac{\sum (t_i - \bar{t})^2 C_i \Delta t_i}{\sum C_i \Delta t_i} = \frac{\sum t_i{}^2 C_i \Delta t_i}{\sum C_i \Delta t_i} - \bar{t}^2 \tag{4.15}$$

$$\frac{\sigma^2}{\bar{t}^2} = 2 \times d - 2 \times d^2 \times \left(1 - e^{\frac{-1}{d}}\right) \tag{4.16}$$

$$E = \frac{CQ_L \bar{t}}{m_t} \tag{4.17}$$

Where:

C : the tracer concentration,

t : time (sec),

Q_L : liquid flow rate

m_t : total mass of tracer

E : the concentration of tracer (dimensionless)

θ : time (dimensionless).

As shown in Table 4.2 and 4.3, there are 16 sets of experiments been conducted to acquire the recovery and t_{10}/HRT. According to the research conducted by Langlais (1991), the t_{10}/HRT could serve as an indicator for channeling in a reactor, indicating that the T value in disinfection was t_{10}. Henry and Freeman (1995) discovered that t_{10}/HRT value would be enhanced as the ratio of liquid height over liquid flow rate increasing in bubble column. For the fixed liquid height in bubble column, the liquid flow rate became the controlling factor on t_{10}/HRT value. From Table 4.2 and 4.3, we could find that t_{10}/HRT and H_L/G_L might have positive relationship. Here was a prediction formula proposed by Marinas et al. (1993) that expressed as following:

$$\log \frac{t_{10}}{\bar{t}} = -2.7 \times \frac{Re_G^{0.25}}{Re_L^{0.83}} \tag{4.18}$$

For discussing diffusion coefficient (d), that was discussed by Ko (1999) and raised an empirical formula for governing d, shown as following:

$$d = 0.00185 + 9.7 \times \frac{Re_G^{0.5}}{Re_L^{1.67}} \tag{4.19}$$

where $Re_G = \frac{U_G d_B}{\nu_L}$ and U_G was the gaseous superfacial flow rate

dB = average diameter of bubble

ν_L = the kinematic viscosity

Pe = Peclet number = $5.72+Re_G^{0.5}Re_L^{1.25}$

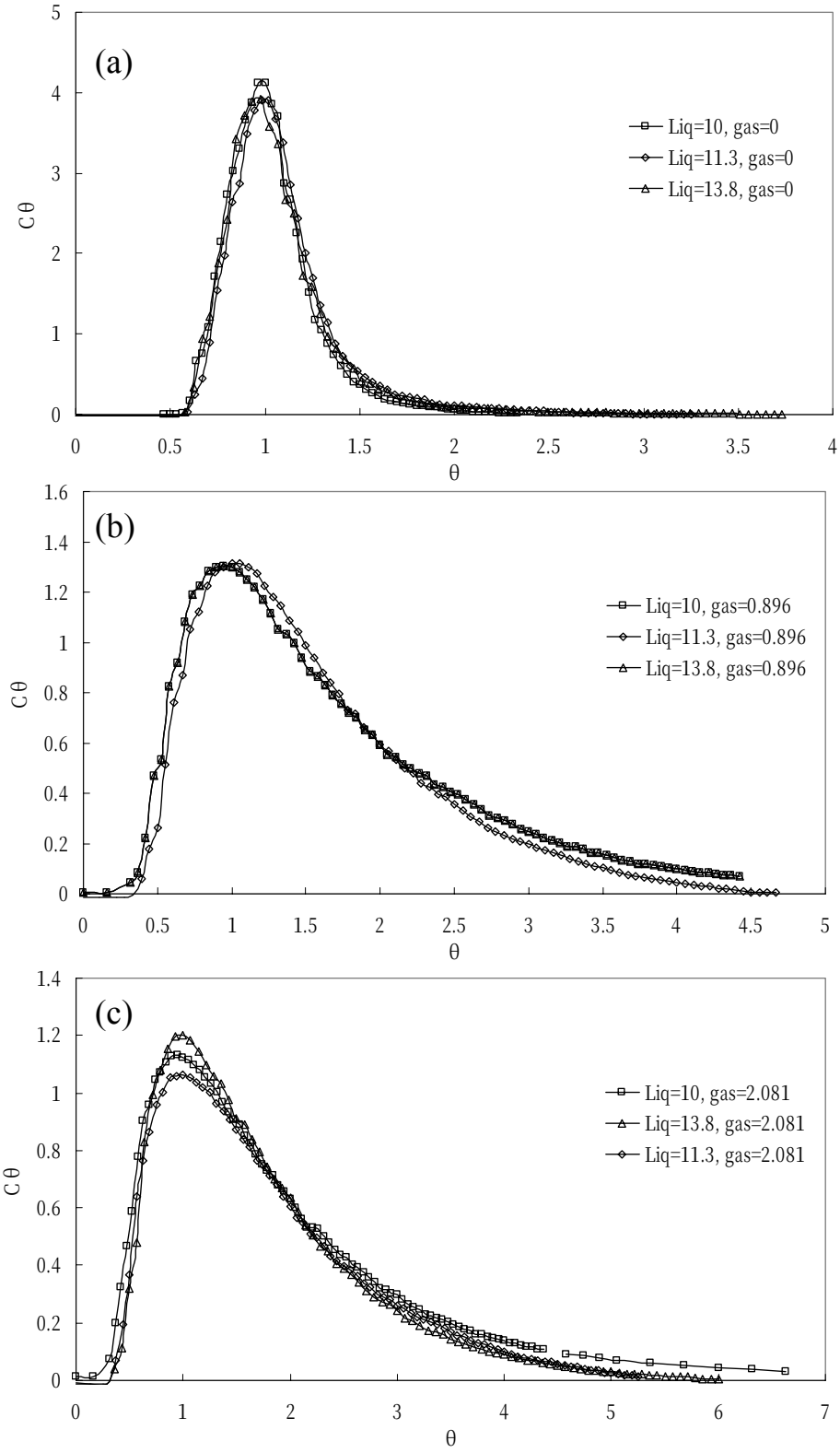

Figure 4.15 The results of tracer test under fixed gas flow rate (G_G). (a) no gas, (b) G_G = 0.9 L/min, (c) G_G = 2.1 L/min

Table 4.2 Tracer test results and parameters for large flow rate patterns

U_L (L/min)	U_G (L/min)	HRT (min)	MRT (min)	t_{10} (sec)	t_{50} (sec)	Recovery (%)	t_{10}/HRT
10	2. 1	4.6	17.3	118	282	103	0.43
	4.6	4.6	17.6	115	270	101.5	0.42
	6.7	4.6	15.02	113	255	90.1	0.41
12	2. 1	3.8	15.7	124	237	101	0.54
	4.6	3.8	14.8	90	199	102	0.39
	6.7	3.8	14.3	83	205	104	0.36
14	2. 1	3.3	13	93	200	104	0.47
	4.6	3.3	12.3	90	190	105	0.45
	6.7	3.3	12.2	71	170	105	0.36

Table 4.3 Tracer test results and parameters for samll flow rate patterns

U_L (L/min)	U_G (L/min)	HRT (min)	MRT (min)	t_{10} (sec)	t_{50} (sec)	Recovery (%)	t_{10}/HRT
2	2.1	23	29	192	720	95	0.14
2.4	0.9	19.2	27.5	315	1242	77	0.27
	2.1	19.2	28.2	246	742	105	0.21
	2.6	19.2	28.6	189	702	105	0.16
	3.2	19.2	25	198	624	104	0.17
4	2.1	8.6	18.6	192	780	107	0.37
6	2.1	7.7	18.5	186	940	115	0.41

4.3.2 Ozoantion of RB 5 in BCR

The variation of pH, $A_{597\ nm}$, color, and TOC for RB 5 at the condition of G_L = 2.4 l/min, G_G = 2.1 l/min, and C_{A0} = 60 g/m^3 are shown in Fig. 4.15. As ozonation proceeded, due to organic and inorganic acids formation, the pH decreased rapidly from 5.5 to 4.0 within 0.5 hydraulic retention time (HRT); as the system approaching to a steady state, the pH reached to a constant (3.8 ± 0.1). The unreacted RB 5 existing in effluent was detected by monitoring the $A_{597\ nm}$, observing that $A_{597\ nm}$ decreased rapidly while conducting ozone-enriched gas into BCR system. The $A_{597\ nm}$ in the effluent was undetectable as HRT > 0.5 that suggested the RB 5 removal efficiency approaching to 100%, suggesting that RB 5 and O_3 is a fast reaction. Due to the high reactivity, azo bond (N=N) may serve as the first place to be attacked by ozone, also, under acidic conditions, ozone dissolved into liquid phase and then reacted with RB 5 molecules whereas the indirect reaction was dominant. The abatement of color changed from 153 IAU to 1.6 IAU within 1 HRT, suggested that most chromophores in liquid phase were destroyed by O_3, and its reduction was similar to RB 5 removal. The TOC reduction was simultaneously with decolorization that decreased from 16 mg/l to 5 mg/l within 1 HRT, and reached to a steady constant (3 mg/l). Clearly, TOC could not be totally removed by ozone in this study because of persistent by-products formed (Chiang, et al., 1999). It is clearly that N=N is more reactive than aromatic ring, it suggested that most O_3 molecules would attack on N=N rather than open aromatic ring and then reduce TOC. As a result, the dissolve ozone concentration ($O_{3,\ diss}$) profile was concerned with the level of decolorization, the profile could be observed after the completion of decolorization, as shown in Fig. 4.16. The appearance of dissolved ozone in effluent indicated that the dissolved ozone utilization rate slowed down and the slower TOC reduction was dominated gradually. The ozone concentration in off-gas ($O_{3,\ off}$) was monitored

simultaneously and its concentration increased swiftly as ozone-enriched gas conducted into system, from none to 15 g/m^3. $O_{3,\ off}$ increased slightly when dissolved ozone started building up, that might due to the decreasing of ozone consumption after totally decolorization. The sulfate and nitrate were the final products of RB 5 by ozone treatment that were consistent with the reduction TOC; sulfate and nitrate concentrations reached 25 and 1.3 mg/l, respectively, after 2 HRT. Referring to the chemical structure of RB 5, one RB 5 molecule contains six sulfate groups and two azo bonds. As ozonation proceeded, sulfate release amount was about 20 times of nitrate formation, suggesting that nitrate formation needed to breakdown the aromatic ring that was a slower reaction comparing to cleavage sulfate from aromatic ring. Similar observation was reported as Chen et al. (2004) studied the oxidation of 2-merceaptothiazoline by ozone and suggested the release of sulfate group is faster than TOC removal and nitrate formation.

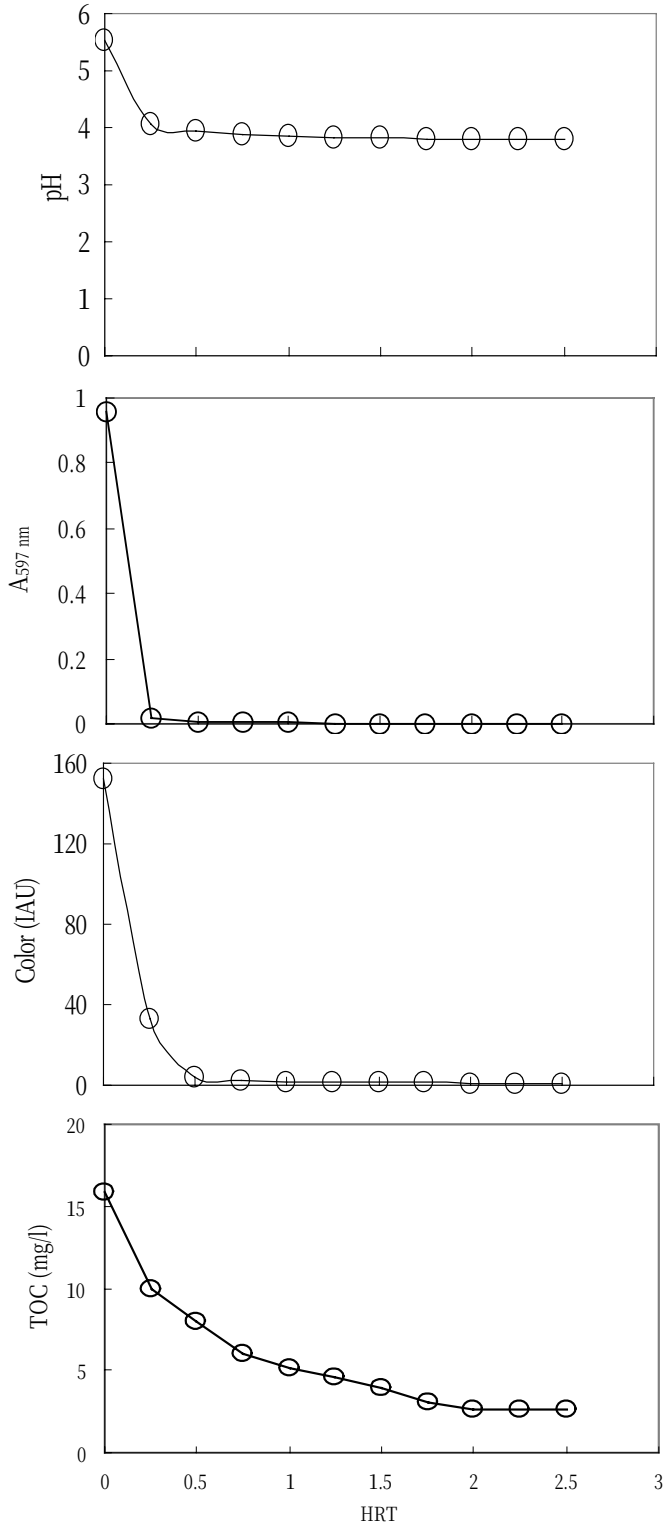

Figure 4.16. The RB 5 ozonation profiles of pH, A_{597nm}, color, TOC, sulfate, and nitrate under the condition of [RB 5] = 50 mg/l, G_L = 2.4 l/min, G_G = 2.1 l/min, C_{A0} = 60 g/m^3, 30 ^oC.

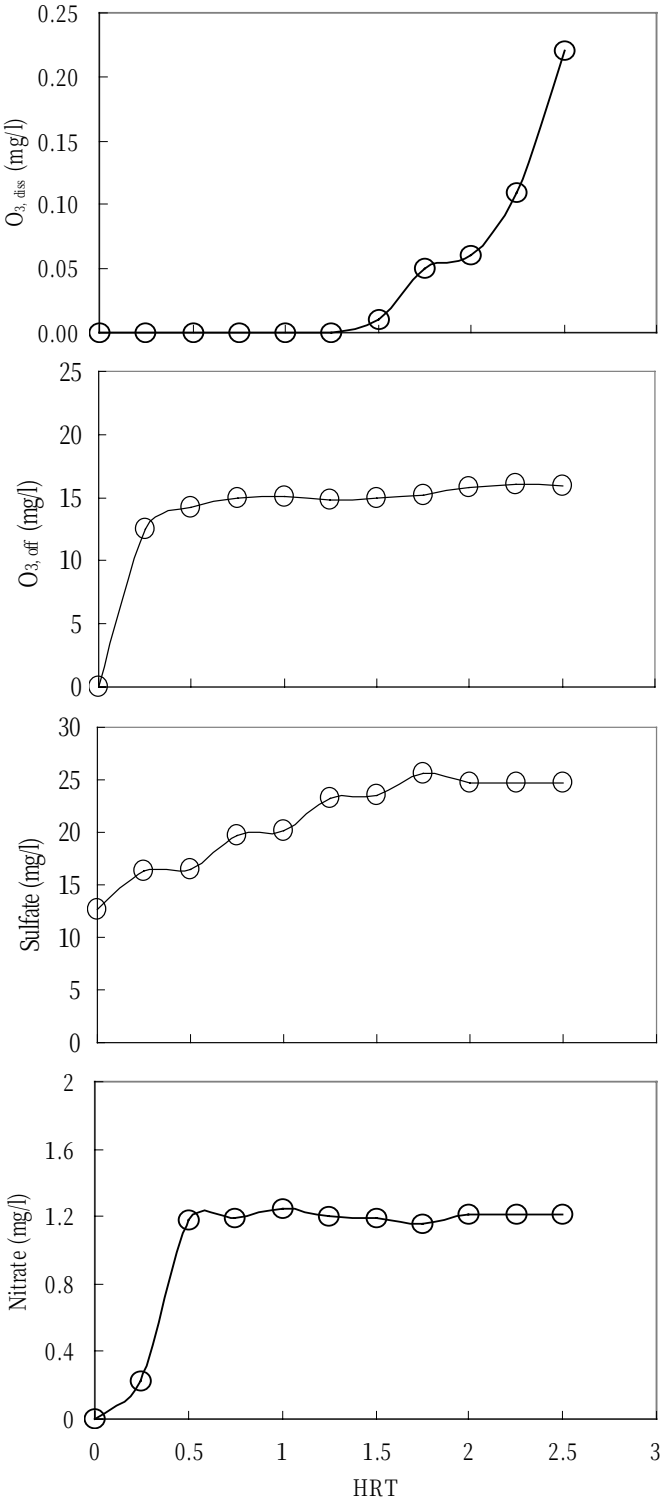

Figure 4.17 The RB 5 ozonation profiles of ozone concentration in liquid and off-gas, sulfate, and nitrate under the condition of [RB 5] = 50 mg/l, G_L = 2.4 l/min, G_G = 2.1 l/min, C_{A0} = 60 g/m^3, 30 ^oC.

4.3.3 The affect of flow pattern on RB 5 ozonation

Fixed liquid flow rate

The variation of decolorization, TOC removal efficiency (η_{TOC}), UV removal efficiency (η_{UV}), and the sulfate yield ($Y_{SO_4^{2-}}$) were monitored at the BCR exist under fixed liquid flow rate (G_L = 2.4 l/min) while changing G_G from 0.9 to 3.4 l/min, the results were showed in Fig. 4.18. For the variation of decolorization, as shown in Fig 4(a), it was clearly that the smaller G_G (0.9 l/min) would result in less decolorization comparing with that of high G_G, and the reduction extent were not proportional to G_G increasing. The results indicated that, as G_G > 2.1 l/min, the G_G was not an important factor to decolorization because the amount of ozone supply was over the need for decolor; which implies that G_G could be an important factor on controlling decolorization under G_L/G_G > 1.14. It suggested that the amount of dissolved ozone ($O_{3,diss}$) provided was not enough to break all the existed azo bonds in water under the conditions of G_G = 0.9 l/min, the corresponding applied ozone dosage (C_{A0} ˙ G_G / V_L) was 1.2 mg/l/min. The η_{TOC} and η_{UV} results, as shown in Fig 4.17(b) and (c), showed the similar increasing pattern, the extents increased as G_G increasing, except for G_G = 0.9 l/min. The η_{TOC} was affected by G_G that could be viewed as applied ozone dose in this study. As G_G increasing, that meant applied ozone dose increasing, the higher G_G the more TOC could be removed that was coincident with the pseudo-first order kinetic model; the amount of η_{TOC} could enhance to 0.9, and the difference between four G_Gs was only 12 %.

The η_{UV} variation may represent the level of unsaturated bonds existing in effluent that may serve as an important factor to evaluate the removal of RB 5 and its derivatives by ozone. For the η_{UV} results shown in Fig. 4.19(c), because of incomplete of decolorization under G_G = 0.9 l/min, the amount of η_{UV} only reached

0.6, it was significant lower than that in other G_Gs. It proved that the certain amount of organics did not ozonate and discharge with effluent, also, it is noted that the η_{UV} for G_G = 2.1, 2.7, and 3.4 l/min existed little difference that echoed the explanation of decolorization. Sulfate formation was consistent with TOC diminishing as aforementioned, and sulfate yield ($Y_{SO_4^{2-}}$) increased as G_G increasing ranging from 0.1 mM (G_G = 0.9 l/min) to 0.15 mM (G_G = 3.4 l/min) and an exponential correlation was suggested strongly between $Y_{SO_4^{2-}}$ and G_G, as shown in Fig. 4.18.

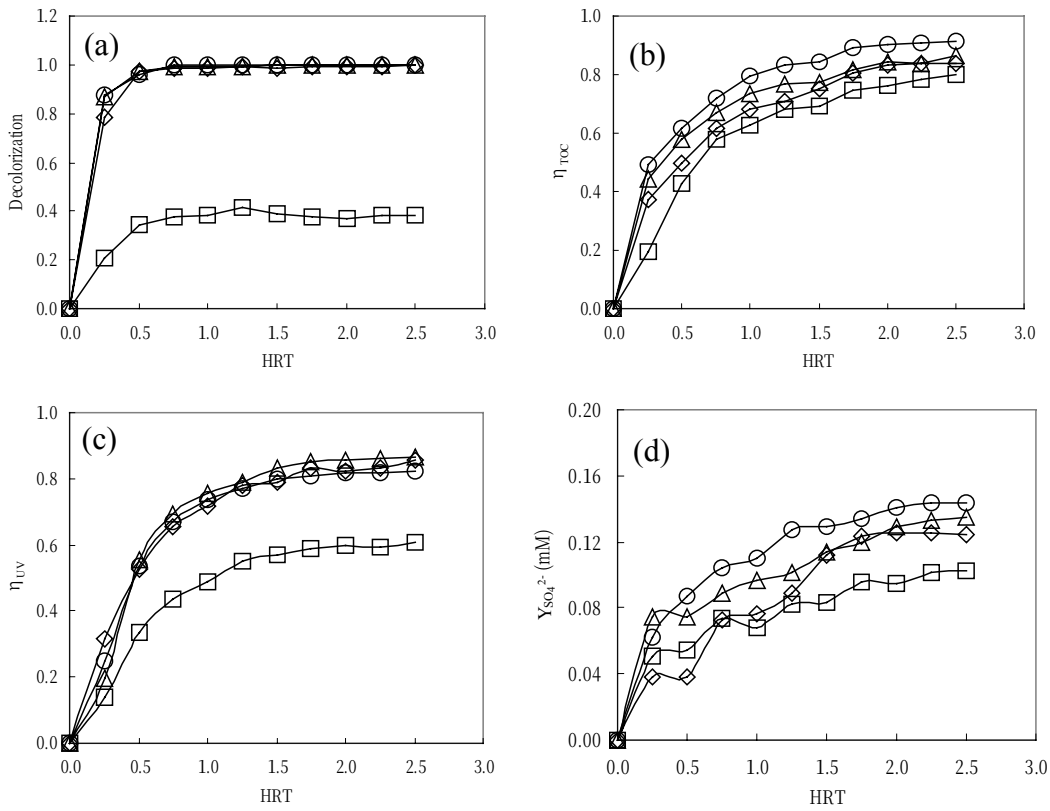

Figure 4.18 The variation profiles of (a) decolorization, (b) η_{TOC}, (C) η_{UV}, and (d) $Y_{SO_4^{2-}}$ at the exist for four different gas flow rate under G_L = 2.4 l/min and C_{A0} = 60 g/m^3 conditions. Notation: □: G_G = 0.9 l/min, ◇: G_G = 2.1 l/min, △: G_G = 2.7 l/min, ○: G_G = 3.4 l/min.

Fixed gas flow rate

Using the similar approaches in fixed liquid flow experiments, fixed ozone-enriched gas flow rate at 2.1 l/min and increasing G_L from 2 to 6 l/min to observe the variation of decolorization, η_{UV}, η_{TOC}, and $Y_{SO_4^{2-}}$, the results were shown in Fig. 4.19. As shown in Fig. 4.19(a), the decolorization for four G_Ls were slightly different among them and all above 0.9; except under the condition of G_L = 6 l/min, the decolorization amounted only 0.7. Comparing the decolorization under the conditions of G_L = 2 and 6 l/min, the difference between them was about 0.28 indicating that ozone dose was not enough to consume the amount of azo bonds under G_L = 6 l/min condition; for other three G_Ls, the difference between each other were not significant. For η_{TOC} measurements, as shown in Fig. 4.18(b), it is found that η_{TOC} reached steady states after 1.5 HRT, the differences among G_L = 2, 4, and 6 (η_{TOC} = 0.86, 0.74, and 0.33 respectively) were remarkable, indicating that η_{TOC} was decreasing as G_L increasing, which meant more pollutants input as fixed ozone dose supply. For the cases of G_L = 2 and 2.4, the average η_{TOC} both over 0.8, it suggested that ozone mass transfer efficiencies in BCR were better than in semibatch reactor as Chen et al. (2003) reported.

As shown in Fig. 4.19(c), it illustrated the η_{UV} variation that suggested correlation between η_{UV} and G_L under fixed G_G conditions. As G_L increasing from 2 to 6 l/min, η_{UV} decreased from 0.78 to 0.28 under fixed G_G, indicating that ozone supply was a significantly controlled factor on η_{UV}. Also, from the dissolved ozone profile by monitoring in the BCR exist showed that no dissolved ozone was monitored at high G_L condition. It is clearly that dissolved ozone was consumed right after its dissolution, and suggesting azo bond could react quickly with ozone molecules. As forementioned, sulfate formation was consistent with TOC reduction

as shown in Fig 4.19(d). It indicated that the extent of $Y_{SO_4^{2-}}$ did not significantly reduce as G_L increasing due to the releasing of sulfate.

The results for comparison of η_{TOC} and $Y_{SO_4^{2-}}$ under fixed G_L and G_G were shown in Fig 4.20. It is observed that the affect of fixed G_G on η_{TOC} was more significant than that of fixed G_L, as well as on the $Y_{SO_4^{2-}}$. While comparing the η_{TOC} vs. G_L/G_G, it is clearly that the η_{TOC} under fix G_G is better than that under fix G_L when $1 < G_L/G_G < 2$. For the conditions of $1 > G_L/G_G$ and $G_L/G_G > 2$, the fix G_G affects are remarkable. It suggested that sulfate formation is consistent with ozone dose, and the extent of $Y_{SO_4^{2-}}$ would be affected by the G_L/G_G variation. As G_L/G_G increasing, η_{TOC} decreased rapidly than $Y_{SO_4^{2-}}$, implying that the rate of sulfate formation might faster than TOC reduction that was proposed by Chen et al. (2004). The detailed parameters are shown in Table 4.4.

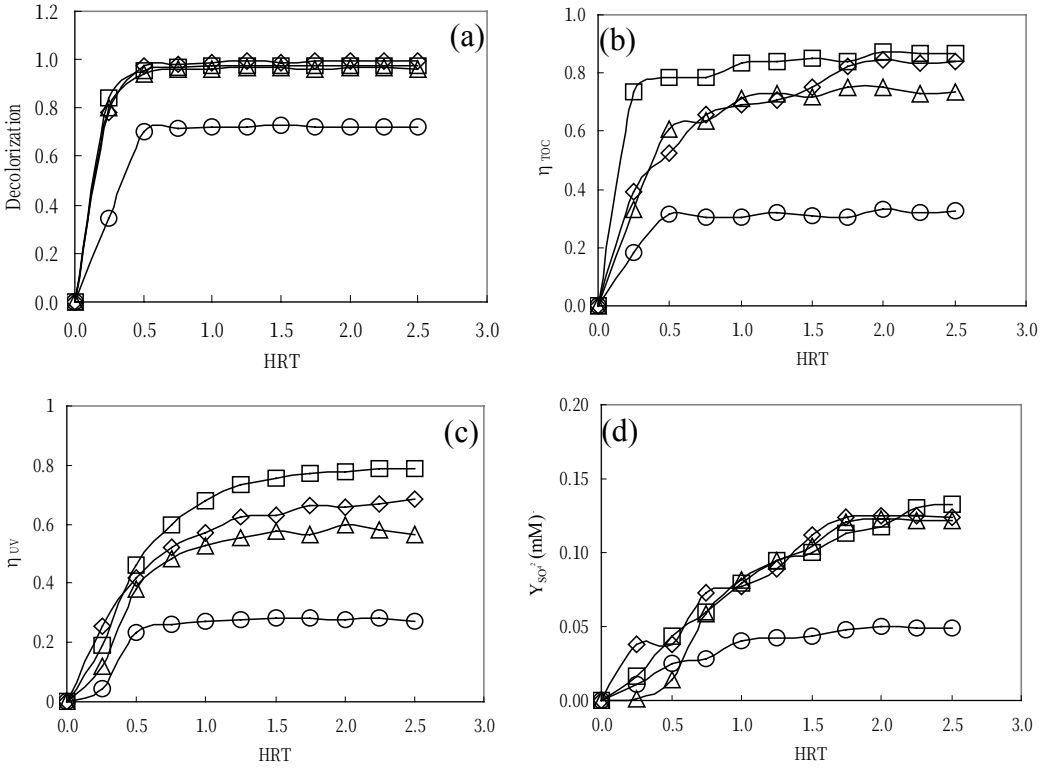

Figure 4.19 The variation profiles of (a) decolorization, (b) η_{TOC}, (C) η_{UV}, and (d) $Y_{SO_4^{2-}}$ at the exist for four different liquid flow rates under G_G = 2.1 l/min and C_{A0} = 60 g/m^3 conditions. Notation: □: G_L = 2.0 l/min, ◇: G_L = 2.4 l/min, △: G_L = 4.0 l/min, ○: G_L = 6.0 l/min.

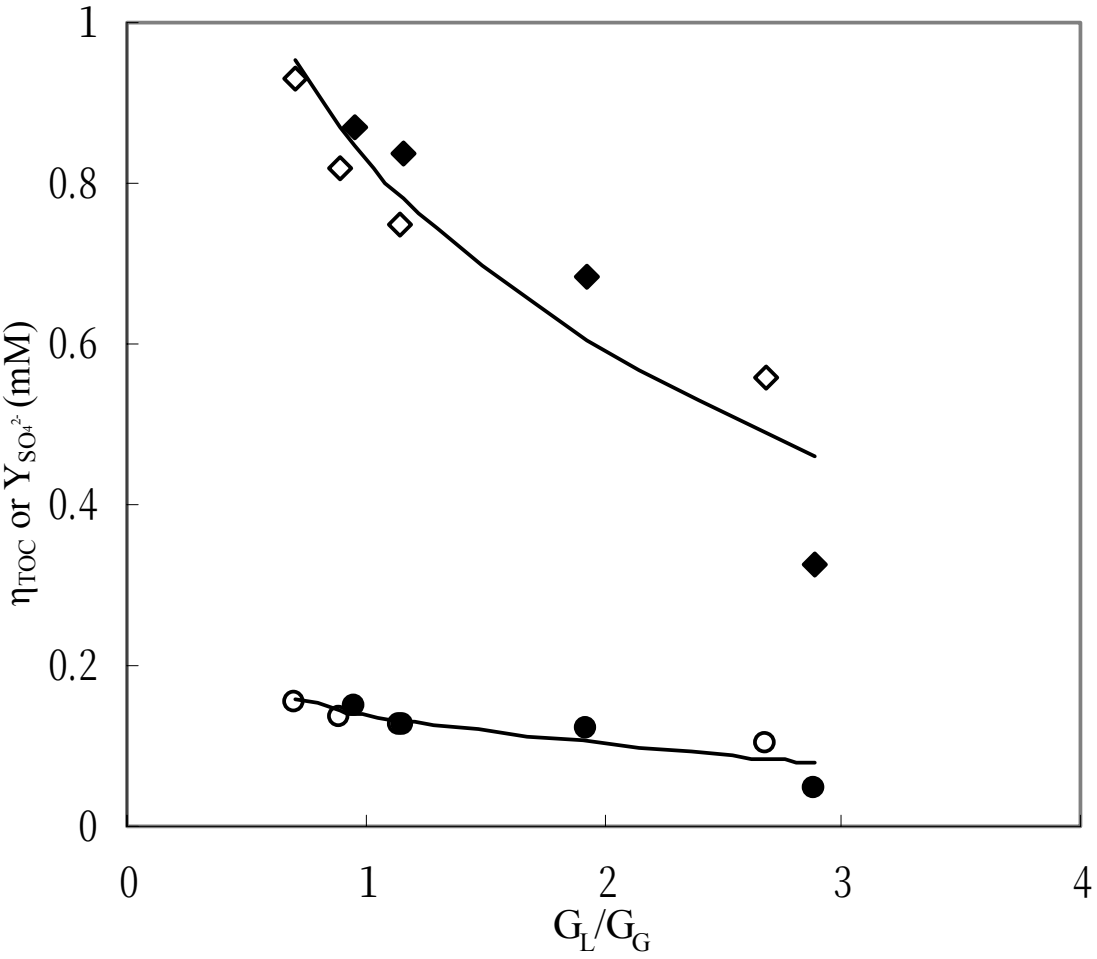

Figure 4.20 The correlation of η_{TOC} and $Y_{SO_4^{2-}}$ vs. G_L/G_G under fixed G_L (2.4 l/min) and G_G (2.1 l/min) with C_{A0} = 60 g/m^3 conditions. Notation: fixed G_L, fixed G_G: ◇, ◆: η_{TOC}, R^2 = 0.89; ○, ●: $Y_{SO_4^{2-}}$, R^2 = 0.76

Ozone consumption associated with TOC removal

By measuring the ozone concentration in the off-gas and effluent at the exit, the ozone consumption (m_{O_3R}) can be calculated as follows:

$$m_{O_3R} = \int_0^t G_G (C_{Ao} - C_{Ae}) dt \qquad (4.20)$$

where C_{Ae} is the ozone concentration at the outlet.

The gas holdup and O_3 gas reacting with ozonated gaseous by-products within the BCR were ignored. As O_3 introduced into BCR, dissolved O_3 was consumed to decolor and remove TOC degradation. For the fixed liquid flow experiments, O_3 supply was not the limiting factor, TOC/TOC_0 followed the first order reaction rate and illustrated as shown in Fig. 4.21. It is found that TOC/TOC_0 decreases with m_{O_3R} remarkably and agreeably in all case under fixed liquid flow rate conditions, indicating a high correlation between the reduction of TOC and m_{O_3R}.

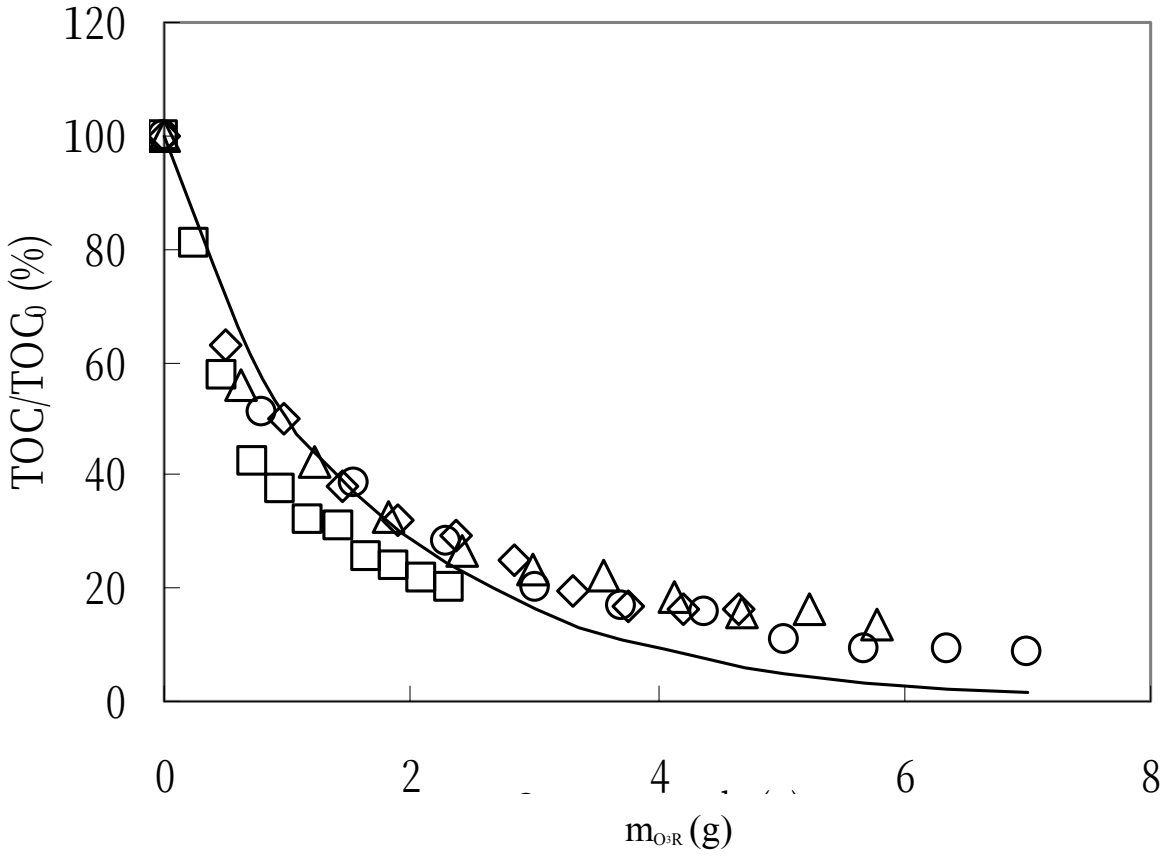

Figure 4.21 The O_3 consumption (m_{O_3R}) vs. TOC/TOC0 variation at fixed liquid flow condition, $R^2 = 0.90$. Notation: □: $G_G = 0.9$ l/min, ◇: $G_G = 2.1$ l/min, △: $G_G = 2.7$ l/min, ○: $G_G = 3.4$ l/min.

For the cases under fixed gas flow rate conditions, the variation of TOC/TOC_0 against m_{O_3R} was shown in Fig. 4.22. Because of the limitation of O_3 supply, the TOC reduction might act as second order reaction rate as expressed by following kinetic equation:

$$dTOC/dt = k[TOC][O_3] \quad (4.21)$$

As seen in Fig. 4.22, the levels of TOC were lowed as m_{O_3R} increasing. It is obvious that liquid flow rate was the controlling factor of TOC reduction, as TOC/TOC_0 went upward as G_L increasing. As the amount of m_{O_3R} approaching 4g, the difference of TOC/TOC0 for high and low reached 23%, indicating that chemical reaction between RB 5 and the amount of dissolved O_3 controlled the TOC reduction rate.

Figure 4.23(a) and (b) showed the effect of ozonation on BOD_5 of two flow patterns, both figures illustrated the positive correlation between BOD_5 and m_{O_3R}. As m_{O_3R} increasing, the BOD_5 increased substantially by about 195 and 225% as m_{O_3R} = 7 and 4.8 g for fixed liquid and fixed gas flow rate conditions, and the rate of BOD_5 increase was a function of m_{O_3R}. The phenomenon could be attributed to the reaction between ozone and RB 5 molecules that opened the long chain high molecular weight and hard-to- biodegradable of RB 5 to the simple biodegradable organic compounds present in the water. Because of low BOD_5 in initial conditions, the effect of ozonation on increasing the BOD_5 of the final ozonated effluent was expected to be high.

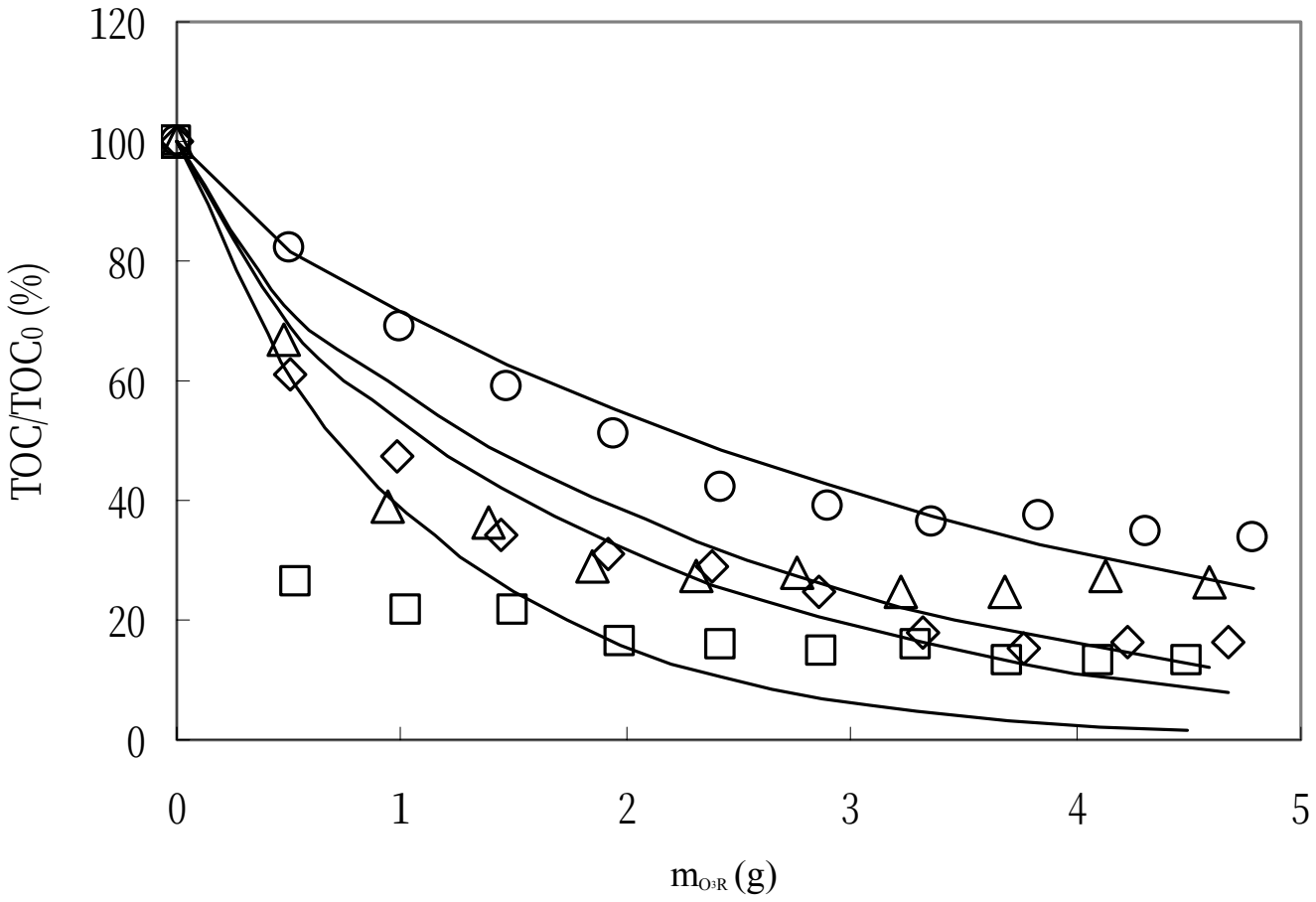

Figure 4.22 The O_3 consumption (m_{O_3R}) vs. TOC/TOC0 variation at fixed gas flow rate conditions. Notation: □: G_L = 2.0 l/min, ◇: G_L = 2.4 l/min, △: G_L = 4.0 l/min, ○: G_L = 6.0 l/min.

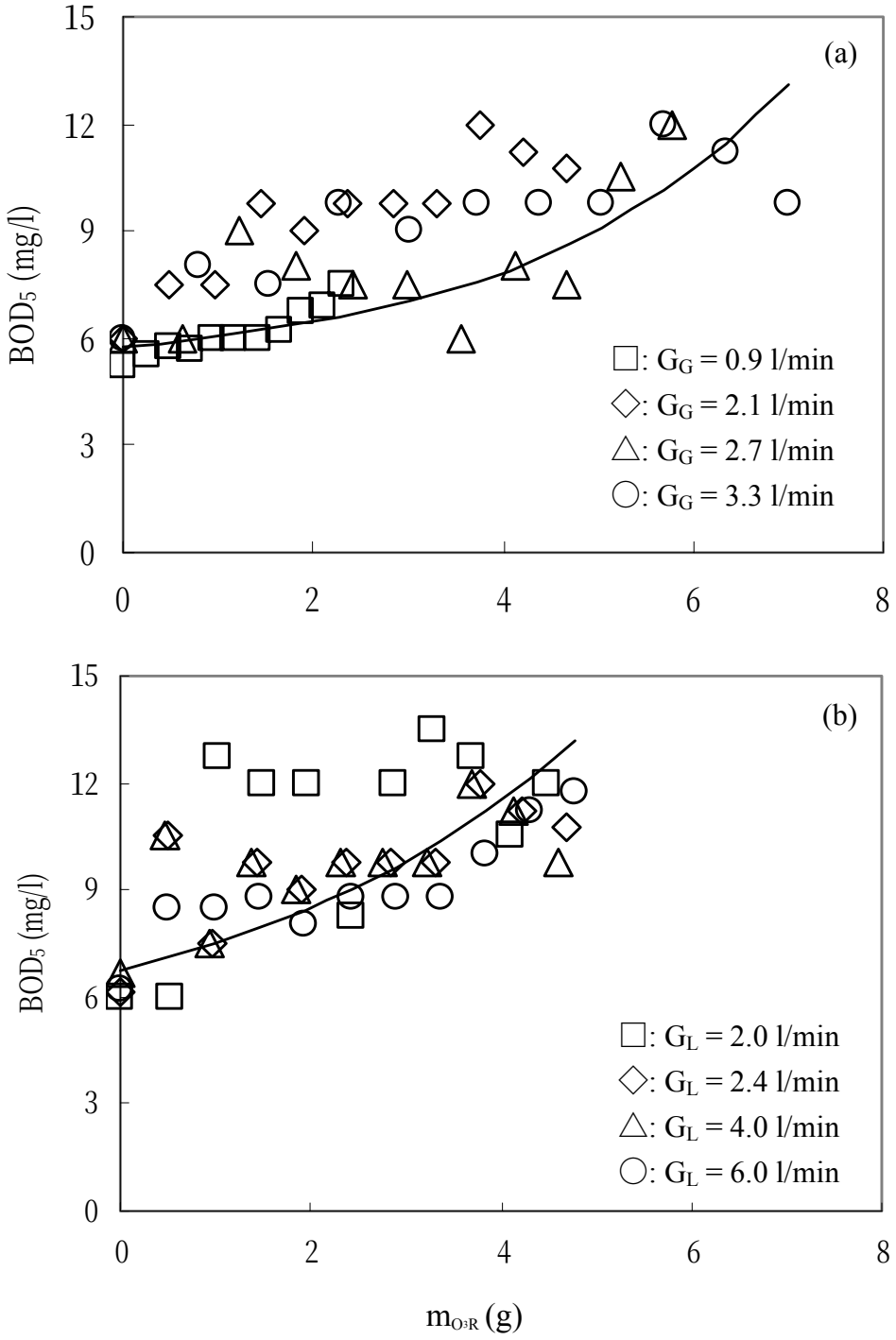

Figure 4.23 The affect of O_3 consumption (m_{O_3R}) on BOD_5 formation. (a) fixed gas flow rate, (b) fixed liquid flow rate.

The column height effect on reducing of color and TOC, and sulfate formation

Since the BCR used in this study was countercurrent flow pattern, liquid flowed downward and ozone-enriched gas flowed upward, the ozone contacting time was affected by column height (H) under both experimental designs. Some investigators have shown that color and TOC reduction concerned with ozonation time and ozone dosage (Perkowski et al., 1996; Konsowa, 2003) as well as column height modeling (Chen et al., 2003). Thus, the variation of color change, TOC reduction, and $Y_{SO_4^{2-}}$ in BCR during ozonation process could be predicted and showed expressed as follows at fixed C_{A0} provided:

Color/Color$_0$ or TOC/TOC$_0$, or $Y_{SO_4^{2-}}$ could be expressed as follows:

$$Y = a \times \left(\frac{G_L}{G_G}\right)^b \times \left(1 - \frac{H}{2.6}\right)^c \qquad (4.22)$$

where Y might represent Color/Color$_0$, TOC/TOC$_0$, or $Y_{SO_4^{2-}}$; a, b, and c were constants; H was the depth of water column. The results of a, b, and c were listed in Table 4. The profile predictions for Color/Color$_0$, TOC/TOC$_0$, or $Y_{SO_4^{2-}}$ of two flow patterns were showed in Fig. 4.24 and Fig. 4.25, respectively. In Fig. 4.24, both color and TOC decreased as gas flow rate increasing while $Y_{SO_4^{2-}}$ increased, indicating that the reduction profiles were controlled by ozone dose. Furthermore, the ozone contacting time, it could be viewed as column height, affected the extent of Color/Color$_0$, TOC/TOC$_0$, and $Y_{SO_4^{2-}}$, observing that the reducing profiles would minimize along with the column height increasing. The results prove that the ozone contacting time relate to ozone consumption in BCR system, taller BCR result in higher ozone consumption. It also suggested that column height could significantly affect the decolorization and mineralization performance in BCR. For the effects of

fixed gas flow rates, it is observed that the reducing extents of Color/$Color_0$ and TOC/TOC_0 are opposite to that under fixed gas flow rate conditions, indicating that the ozone supply is a limiting factor and the effect of column height may act an important factor in controlling the profiles of Color/$Color_0$ and TOC/TOC_0 reduction, as well as the increment of $Y_{SO_4^{2-}}$.

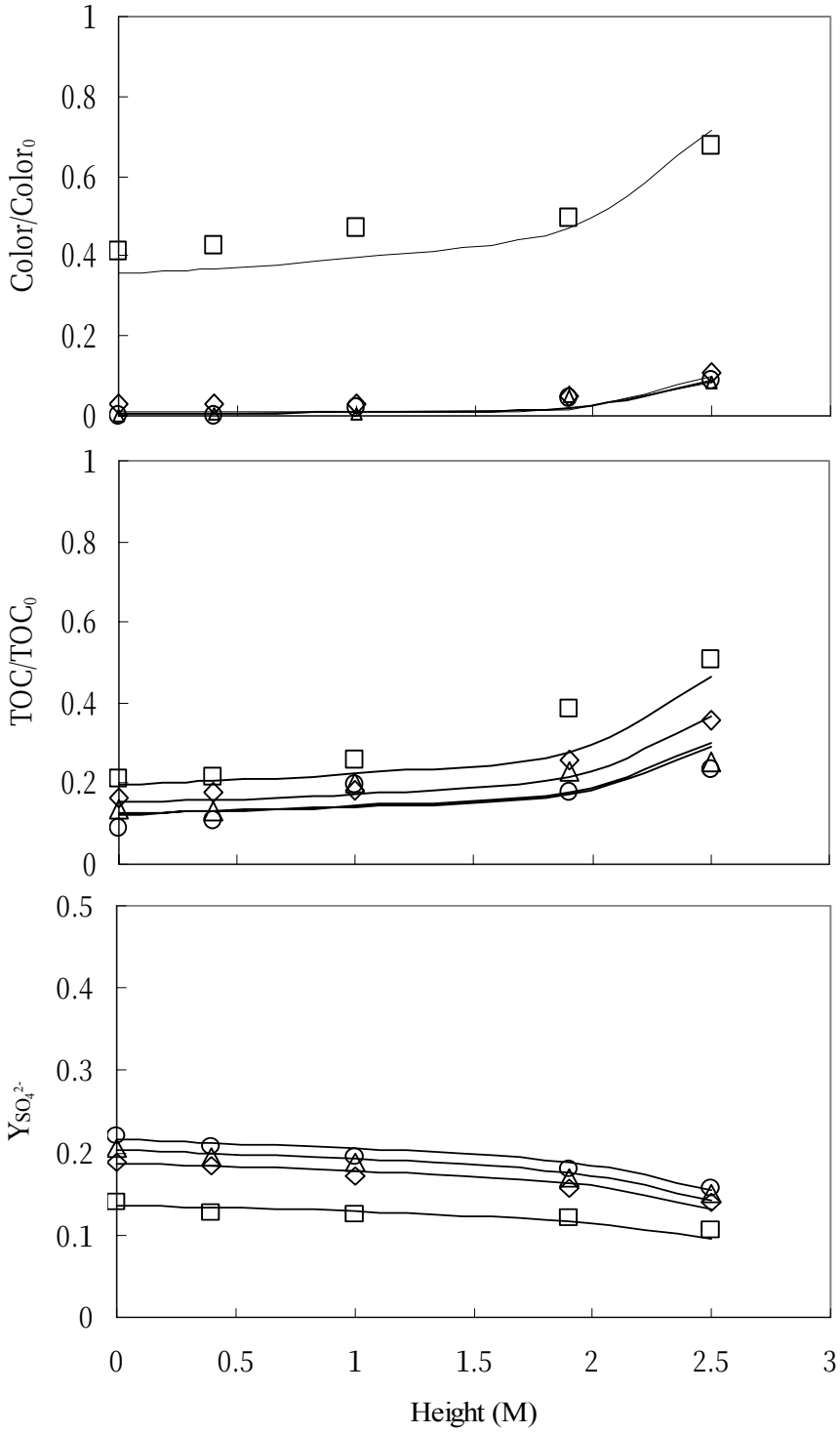

Figure 4.24 The prediction profile for Color/Color$_0$, TOC/TOC$_0$, or $Y_{SO_4^{2-}}$ at 2.5 HRTs under fixed liquid flow condition. Notation: □: G_G = 0.9 l/min, ◇: G_G = 2.1 l/min, △: G_G = 2.7 l/min, ○: G_G = 3.4 l/min.

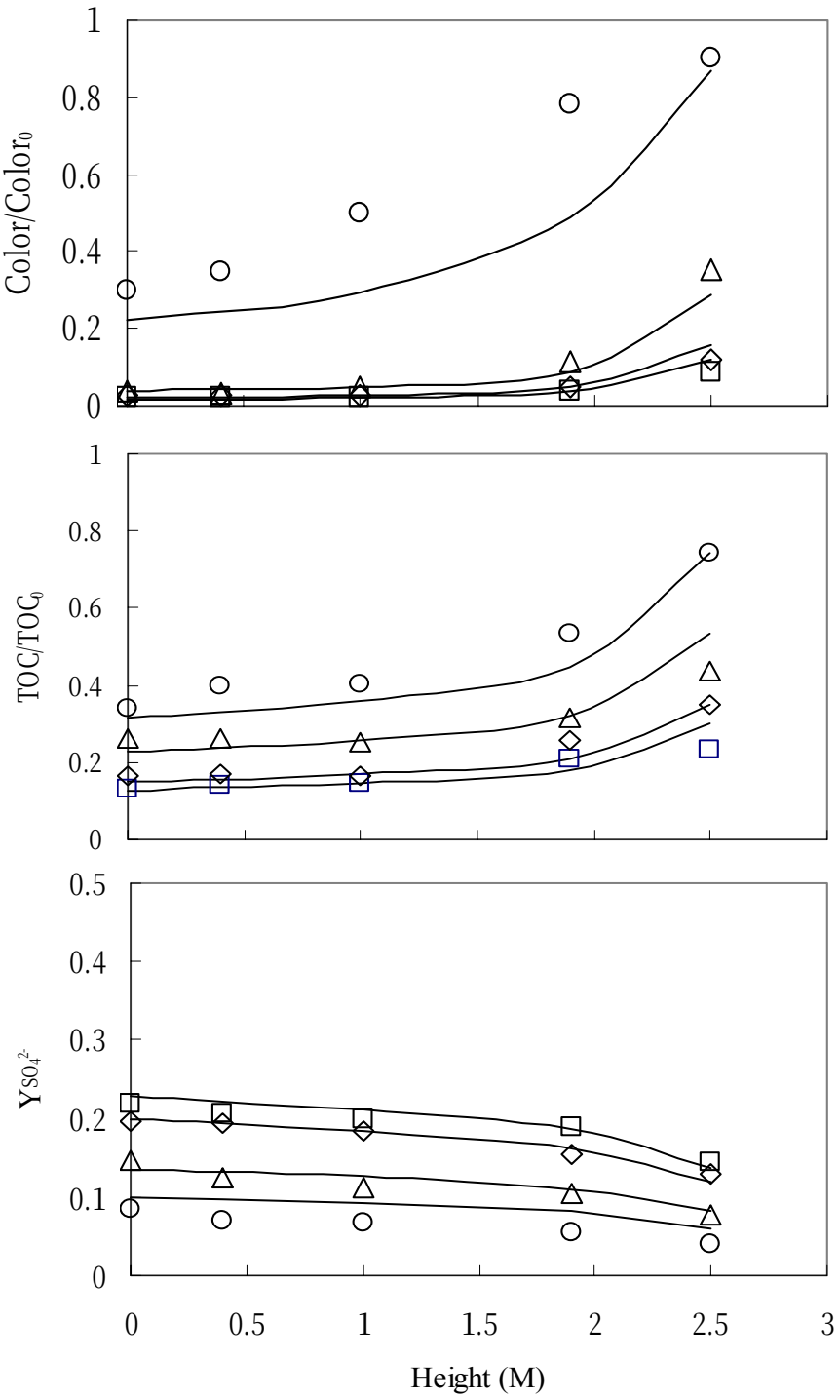

Figure 4.25 The prediction profile for $Color/Color_0$, TOC/TOC_0, or $Y_{SO_4^{2-}}$ at 2.5 HRTs under fixed gas flow rate conditions. Notation: □: G_L = 2.0 l/min, ◇: G_L = 2.4 l/min, △: G_L = 4.0 l/min, ○: G_L = 6.0 l/min.

Table 4.4 The experimental setup and monitored parameters at 2.5 HRT

G_G (l/min)	G_L (l/min)	**Ozone dose** (mg/l-min)	Decolor	η_{TOC}	$[O_3]_{diss}$ (mg/l)
2.1	2	2.4	0.98	0.87	0.88
2.1	2.4	2.4	0.98	0.83	0.22
2.1	4	2.4	0.96	0.73	0
2.4	6	2.4	0.70	0.66	0
0.9	2.4	1.0	0.50	0.79	0
2.7	2.4	3.1	1.00	0.86	0.56
3.3	2.4	3.8	1.00	0.90	0.9

Table 4.4 Parameters estimate for Equation (3).

	a	b	c	R^2
$Color/Color_0$	0.0127	-2.78	-0.606	0.83 (40)*
TOC/TOC_0	0.149	-0.686	-0.220	0.86 (40)*
$Y_{SO_4^{2-}}$	0.198	0.123	0.671	0.80 (40)*

*The number in the parenthesis indicates the samples size.

5. Conclusion and future work

The ozonation of azo dyes both in semibatch reactor and continuous bubble column reactor are investigated in this study. The results reveal the following conclusions:

1. The decolorization of target compound in solution is consistently with applied ozone dose (C_{AGi0}) that is the same in both semibatch reactor and continuous bubble column reactor. The completion of decolorization may also serves as an indicator of accumulation of dissolved ozone commenced.
2. The reaction rate for decolorization is faster than that of TOC reduction, which can be observed during the experimental processes. And, as dimensionless TOC concentration > 0.9 in semibatch system, the dissolved ozone concentration is nearly not detectable, suggesting that most ozone transfer from gas phase to liquid phase is consumed rapidly in oxidizing the azo dye by breaking the azo bond (N=N).
3. In semibatch experiments, both ozone alone and O_3scombined with UV irradiation are used to investigate the effectiveness of deolorization and mineralization of AO 6, the target compound. The results show that O_3/UV system may reach the level of total mineralization of AO 6 within 120 min, also revealing that the O_3/UV system is a powerful treatment to breakdown all organic carbon in solution. But, as consideration of treatment cost, the O_3/UV system may not be the best way to treat textile wastewater. Because that system may need long treatment time and consume more energy.
4. As monitoring the selected parameters during the semibatch experiments, decolorization, and TOC removal were affected by pH, temperature, and ozone dose. Decolorization and AO 6 reduction were completed within 40 minutes of ozonation time for all examined cases. When the ozone dose increased from 2.7 to 3.5 mg/l-min, the decolorization rate constant increased from 0.14 to 0.27 min^{-1}. The increases of k values suggest that decolorization and AO6 removal were affected by ozone dose. For the TOC removal, its reaction rate constants were temperature dependent and

the effects of ozone dose and pH were not significant. Sulfate yield was accelerated upon the completion of decolorization. The sulfate yield may be due to the destruction of azo bonds and surplus ozone or OH^- turns to attack aromatic rings. Significant increment of sulfate yield was observed during the TOC removal process.

5. Other findings in semibatch system regarding the change of selected parameters, conclusions can be made as following: (1) the decolorization of AO 6 dye was affected by ozone dose and pH; however, the effect of temperature contribution on apparent rate constant was limited. (2) TOC removal was affected by temperature significantly, but the affects of pH and ozone dose were limited. (3) Significant increment of sulfate yield was observed upon the completion of decolorization. (4) When the TOC removal > 0.4, sulfate yield was accelerated.

In the countercurrent flow bubble column system,

1. In the BCR system, the ozonation of RB 5 is monitored and the variations are recorded, the results illustrating that may be controlled by the flow rates of liquid and/or gas. The trend shows as a pseudo-first order or second order reaction types depending upon the controlled flow.
2. It is noted that the monitored parameters all achieve to constants as the system approaching to a steady state for TOC, sulfate, and nitrate, but the variations of pH, A597 nm, and color all reach steady constants at 1 HRT. It suggests that color and N=N are easily to be removed comparing to TOC; the sulfate formation is consistent with TOC reduction.
3. The controlled flow may affect the order of reaction, a pseudo-first order reaction is suggested in the fixed liquid flow rate experiments and a second order reaction may well explain for the fixed gas flow rate conditions. Not only flow patterns affect the RB 5 removal and the mineralization of derivatives but also the column height may have influence on the ozone consumption.
4. It is observed that the extent of decolorization and mineralization decrease as the sampling port height increasing, indicating that the column height may reflect the retention time of ozone gas and the

contacting time between ozone and RB 5 in BCR system. The biodegradability is enhanced via ozone treatment that is not proportional to the amount of ozone consumption but all results exhibit the similar increment trends.

5. Due to the column height and flow pattern affects, an experimental regression model is proposed in this study that the variations of $Color/Color_0$, TOC/TOC_0, and can be predicted under such conditions. The R2 values are all above 0.8.

In order to have more integrated study outcome, following work may need to be considered in near future that include:

1. To simulate and verify the experimental results by using sophisticated predict models that are developed by Prof. Chang's team. The models will be modified and/or simplified beforehand, then, to predict the trends of selected parameters.
2. To use the BCR system and simulation model to study the effects of enhancement of ozone and retardant of oxygen.
3. To consider other advanced oxidation processes, such as photo-induced oxidation, catalyst with H_2O_2/UV, photocatalytic adsorption and oxidation, to be adopted in further researches and extended the capacity.

Reference

1. Akmehmet-Balcioğlu I. and Getoff, N (1997) Advanced oxidation of 4-Chlorobenzaldehyde in water by UV-light, ozonation and combination of both methods Chemosphere, 36(9), 1993-2005.
2. American Public Health Association (APHA), Standard Methods for the examination of Water and Wastewater, 19th Ed. (Washington, D.C. : American Public Health Association, 1995)
3. Arora, M.L., Barth, E.F. and Umphres, M.B. (1985) Technology evaluation of sequencing batch reactors. Journal WPCF, 57(8), 867-875.
4. Andreozzi, R. and Marotta, R. (1999) Ozonation of p-Chlorophenol in aqueous solution J. of Hazardous Material, B69, 303-317
5. Arslan, I. and Balcioglu, A. (2000) Effect of common reactive dye auxiliaries in the ozonation of dyehouse effluents containing vinylsulphone and aminochlorotriazine dye Desalination, 130, 61-71
6. Beltràn, F.J., Gomez-Serrano, V. and Duran, A. (1992) Degradation kinetics of p-Nitorphenol ozonation in water Water Research, 26(1), 1309-1316
7. Beltràn, F.J., Gonzàlez, M. and Gonzàlez, J.F. (1997) Industrial wastewater advanced oxidation. Part 1. UV radiation in the presence and absence of hydrogen peroxide or UV radiation Water Research, 31(10), 2405-2414
8. Beltràn, F.J., Encinar, J.M. and Gonzàlez, J.F. (1997) Industrial wastewater advanced oxidation. Part 2. Ozone combined with hydrogen peroxide or UV radiation Water Resource, 31(10), 2415-2428
9. Beltràn, F.J. (1997) Theoretical aspects of the kinetics of competitive first reactions of O3/H2O2 and O3/UV oxidation processes Ozone Science and Engineering, 19(1), 13-38

10. Beltràn, F.J., Beltràn-Heredia, J., Torregrosa, J. and Acero, J.L. 1999. Treatment of olive mill wastewaters by ozonation, aerobic degradation and the combination of both treatment J. of Chemical Technology & Biotechnology, 74(7), 639-646
11. Beltràn, F.J., Garcia-Araya, J.F., Alvarez, P.M. 1999. Integration of continuous biological and chemical (ozone) treatment of domestic wastewater: 1. Biodegradation and post-ozonation. J. of Chemical Technology & Biotechnology, 74(9), 877-883
12. Beltràn, F.J., Beltràn-Heredia, J., Acero, J.L., Rubio, F.J. (2000) Rate constants for the reactions of ozone with chlorophenols in aqueous solutions J. of Hazardous Material, B79, 271-285
13. Beltràn, F.J., Beltràn-Heredia, J., Acero, and Rubio, F.J. (2000) Contribution of free radicals to chlorophenols decomposition by several advanced oxidation processes Chemosphere, 41, 1271-1277
14. Chen, L.-C. (2000) Effects of factors and interacted factors on the optimal decolorization process of methyl orange by ozone. Water Research, 34(3), 974-982.
15. Chen, Y.H., C.Y. Chang, C.C. Chen, C.Y. Chiu, Y.H. Yu, P.C. Chiang, C.F. Chang, and Y. Ku "Decomposition of 2-Mercaptothiazoline in an Aqueous Solution by Ozoantion with UV Radiation" Ind. Eng. Chem. Res. 43(9): 1932-1937 (2004).
16. Chiang, P. C., Ko,Y-W. Liang, C.-H., and Chang, E.E. (1998) Modeling an ozone bubble column for predicting its disinfection efficiency and control of disinfection by-products formation Chemosphere, 39(1), 55-70
17. Chu, W. and Ma, C.-W. (1998) Reaction kinetics of UV-decolorization for dye materials Chemosphere, 37(5), 961-974
18. Chu, W. and Ma, C.-W. (2000) Quantitative prediction of direct and indirect dye ozonation kinetics. Water Research, 34, 3153-3160

19. Cogo,E., Albet, J., Malmary, G., Coste, C. and Molinier, J. (1999) Effect of reaction ozone mass transfer and applications to pulp bleaching Chemical Engineering Journal, 73, 23-28.
20. European Union, European Union Council Directive 2003/53/EC amending for the 26th time Council Directive 76/769/EEC relating to restrictions on the marketing and use of certain dangerous substances and preparations (nonylphenol, nonylphenol ethoxylate and cement). Off. J. European Union, L 178/24-L 178/28 (2003).
21. Glaze W.H. and G.R. Peyton, "Destruction of Pollutants in Water with Ozone in Combination with Ultraviolet Radiation. 3. Photolysis of Aqueous Ozone" Environ. Sci. Technol. 22(7): 761–767 (1988).
22. Gottschalk, C., J.A. Libra, and A. Saupe, Ozonation of Water and Wastewater-Apractical Guide to Understanding Ozone and Its Application. (Gmbh, Weinhein, Germany: Wiley-VCH, Verlag, 2000), p. 12-15.
23. Gurol; M. and Singer, P. (1982) Environmental Science and Technology, 16(7):377-383
24. Hao, O. J.; Kim, H.; and P. Chiang (2000) Decolorization of wastewater. Critical Reviews in Environmental Science and Technology, 30(4), 449-505.
25. Hautaniemi, M., J. Kaalas, R. Munter, and M. Trapido, "Modeling of Chlorophenol Treatment in Aqueous Solutions. 1. Ozonation and Ozonation Combined with UV Radiation Under Acidic Conditions" Ozone: Sci.Eng. 20(4): 259-282 (1998).
26. Hermanowicz, S.W., Bellamy, W.D. and Fung, L.C. (1999) Variabilty of ozone reaction kinetics in batch and continuous flow reactors Water Research, 33(9), 2130-2138
27. Hitchcock,D.R., Law, S.E., Wu, J. and Williams, P.L. (1998) Determining

toxicity trends in the ozonation of synthetic dye wastewaters using the Nemaode *Caenorhabditis elegans*. Archives of Environmental Contamination and Toxicity, 34, 259-264.

28. Hostachy, J.-C., Lenon,G., Pisicchio, J.-L., Coste, C. and Legay, C. (1997) Reduction of pulp and paper mill pollution by ozone treatment Water Science and Technology, 35(2-3), 261-268
29. Huang, C.-R. and Shu, H.Y. (1995) The reaction kinetics, decomposition pathways and intermediate formation of phenol in ozonation, UV/O3 and UV/H2O2 processes J. of Hazardous Material, 14, 47-64
30. Ikemizu, J., Morooka, S., Kato, Y. (1987) Decomposition rate of ozone in water with ultraviolet radiation J. Chemical Engineering, Japan, 20(1), 77-81.
31. Kasprzyk-Horden B., M. Ziółek, and J. Nawrocki "Catalytic Ozonation and Methods of Enhancing Molecular Ozone Reactions in Water Treatment" Appl. Catal., B: 46(4), 639-669 (2003).
32. Koch, M., A. Yediler, D. Lienert, G. Insel, and A. Kettrup, "Ozonation of Hydrolyzed Azo Dye Reactive Yellow 84 (C.I.)" Chemosphere, 46(1): 109-113 (2002).
33. Ku, Y., Su, W.J., and Shen, Y.S. (1996) Decomposition kinetics of ozone in aqueous solution Industrial Engineering and Chemical Resource 35(10), 3369-3374
34. Kuo, W.S. (1999) Synergistic effects of combination of photolysis and ozonation on destruction of chlorophenols in water Chemosphere, 39(11), 1853-1860
35. Langlais, B., Reckhow, D.A. and Brink, D.R. (1991) Ozone in water treatment—Application and Engineering Lewis Publishers.
36. Ledakowicz, A.; Solecka, M; and Zylla, R. (2001) Biodegradation, decolorization and detoxification of textile wastewater enhanced by advanced

oxidation processes. J. of Biotechnology, 89, 175-184.

37. Lopez, A,. Ricco, G., Ciannarella, R., Rozzi, A., Di Pinto, A.C. and Passino, R. (1999) Textile wastewater reuse: ozonation of membrane concentrated secondary effluent Water Science Technology, 40(4-5), 99-105
38. Martins, M.A.M.; Ferreira, I.C.; Santos, I.M.; Queiroz, M.J.; and Lima, N. (2001) Biodegradation of bioaccessible textile azo dye by *Phanerochaete chrysosporium*. J. Biochnology, 89, 91-98
39. Nitschke, L.; Wilk, A.; Schussler, W.; Metzner, G.; Lind,G. (1999) Biodegradation in laboratory activated sludge plants and aquatic toxicity of herbicides. Chemosphere, 39(13), 2313-2323
40. Oeller, H.-J., Demel, I. and Weinberger, G. (1997) Reduction in residual COD in biologically treated paper mill effluents by means of combined ozone and ozone/UV reactor stage. Water Science Technology, 35, 269-276
41. O'Neill, C., Hawkes, F.R., Esteves, S.R.R., Hawkes, D.L. and Wilcox, S.J. 1999. Anaerobic and aerobic treatment of a simulated textile effluent. J. of Chemical Technology & Biotechnology, 74(10), 993-999.
42. Oliviero L., J. Barbier and D. Duprez "Wet Air Oxidation of Nitrogen-containing Organic Compounds and Ammonia in Aqueous Media" Appl. Catal., B. 40 (3): 163-184 (2003).
43. Parisheva, Z. and Demirev, A. (2000) Ozonation of ethanolamine in aqueous medium Water Research, 34(4), 1340-1344
44. Qiu, Y. (2001) Performance and simulation of ozone absorption and reaction in a stirred-tank reactor Environmental Science and Technology 2001, 35, 209-215
45. Rajaguru, P., Kalaiselvi, K., Palanivel, M., and Subburam, V. (2000) Bidegradation of azo dyes in a sequential anaerobic-aerobic system. Applied Microbial Biotechnology, 54, 268-273.

46. Rathi A., H.K. Rajor, and R.K. Sharma, “Photodegradation of direct yellow-12 using UV/H_2O_2/Fe^{2+}” J. Hazard. Mater. B102: 231-241 (2003).

47. Rice, R.G.; L., Bollky, J.; and Lacy, W.J. (1986) Analytical aspects of ozone treatment of water and wastewater Lewis Publisher

48. Rice, R.G. (1997) Application of ozone for industrial wastewater treatment – A review Ozone Science and Engineering, 18, 477-515

49. Rivas, F.J., Beltràn, F.J., Gimeno, O. 2000. Joint treatment of wastewater from table olive processing and urban wastewater. Integrated ozonation- aerobic oxidation. Chemical Engineering & Technology, 23(2), 177-181.

50. Sakkas V.A and T.A. Albanis, “Photocatalyzed Degradation of the Biocides Chlorothalonil and Dichlofluanid over Aqueous TiO2 Suspensions” Appl. Catal., B. 46(1): 175-188 (2003).

51. Sarasa, J., Roche, M.P., Ormad, M.P., Gimeno, E., Puig, A. and Ovelleiro, J.L. (1998) Treatment of a wastewater resulting from dye manufacturing with ozone and chemical coagulation Water Research, 32(9), 2721-2727.

52. Sevimli M.F.and H.Z. Sarikaya, “Ozone Treatment of Textile Effluents and Dyes: Effect of Applied Ozone Dose, pH and Dye Concentration” J. Chem. Technol. Biotechnol. 77(7): 842-850 (2002).

53. Shenai, V.A. (1976) Technology of Textile processing—Chemistry of Textile Auxiliaries.

54. Shu, H.Y. and Huang, C.-R. (1995) Degradation of commercial azo dyes in water using ozonation and UV enhanced ozonation process Chemosphere, 31(8), 3813-3825

55. Sotelo, J.L.; Beltran, F.J.; Beltran-Heredia, J. (1987) Ozone decomposition in water: kinetics study. Industrial engineering and Chemical Resources, 26, 39-50.

56. Sotelo, J.L.; Beltran, F.J.; Benitez, F.J.; Beltran-Heredia, J. (1989) Henry’s law

constant for ozone-water system. Water Research, 23, 1239-1248.

57. Stockinger, H., Kut, O.M. and Heinzle, E. (1996) Ozonation of wastewater containing n-methylmorpholine-n-oxide Water Research, 30(8), 1745-1748

58. Sumathi, S. and Manju, B.S. (2000) Uptake of reactive dyes by Aspergillus fetidus. Enzyme and Microbial Technology, 27, 347-355.

59. Trapido, M., Hirvonen, A., Veressinina, Y., Hentunen, J., and Munter, R. (1997) Ozonation, ozone/UV and UV/H2O2 degradation of chlorophenols Ozone Science and Engineering, 19(1), 75-96.

60. Wang, C., A. Yediler, D. Lienert, Z. Wang, and A. Kettrup, "Ozonation of an Azo Dye C.I. Remazol Black 5 and Toxicological Assessment of its Oxidation Products" Chemosphere, 52(7): 1225-1232 (2003).

61. Waring, D.R. and G. Hallas, The Chemistry and Application of Dyes (New York, NY: Plenum Press, 1990), p. 18-21.

62. Weiss,L. (1935) Investigatuion on the radical HO2 in solution. Transaction of Far. Sciences, 31, 668.

63. Wu, J. and T. Wang, "Ozonation of Aqueous Azo Dye in a Semi-batch Reactor" Water Res. 35(4): 1093-1099 (2001).

64. Zgajnar, A. and Zagoc-Koncan, J. (1999) Biodegradation studies as an important way to estimate the environmental fate of chenmicals. Water Science and Technology, 39(10-11), 375-382.

65. 染料與助劑名錄，1997 年版 染化雜誌社印行。

66. 胡思聰 (1994) 臭氧預處理之氯酚化合物廢水對於活性污泥系統處理效應之影響 博士論文，國立台灣大學。

67. 柯雅雯 (1999) 臭氧處理對自來水中消毒副產物與有機前質之去除研究 博士論文，國立台灣大學。

68. 申永順 (1998) 以高級氧化程序處理揮發性有機污染物反應行為及光反應

器設計之研究　博士論文，國立台灣科技大學。

69. 中國技術服務社(1992)　加強「染料、助劑對環境污染之影響」研究綜合報告

70. 經濟部工業局 (1997)　工業減廢技術手冊-顏料工業

71. 北原文雄、玉井康雄、早野茂夫、原一郎 (1979)　界面活性劑應用實務，復漢出版社